Transportation Research Part B 138 (2020) 23–45

Contents lists available at ScienceDirect

Transportation Research Part B

journal homepage: www.elsevier.com/locate/trb

Dynamic optimization strategies for on-demand ride services platform: Surge pricing, commission rate, and incentives

Xiqun (Michael) Chen[a], Hongyu Zheng[a,b], Jintao Ke[c], Hai Yang[c,*]

[a] College of Civil Engineering and Architecture, Zhejiang University, 866 Yuhangtang Rd, Hangzhou 310058, PR China
[b] Department of Civil and Environmental Engineering, Northwestern University, 2145 Sheridan Road, Evanston, IL 60208, USA
[c] Department of Civil and Environmental Engineering, The Hong Kong University of Science and Technology, Clear Water Bay, Kowloon, Hong Kong, PR China

ARTICLE INFO

Article history:
Received 17 July 2019
Revised 3 April 2020
Accepted 3 May 2020

Keywords:
On-demand ride services
Surge pricing
Commission rate
Incentives
Dynamic vacant car-passenger meeting

ABSTRACT

On-demand ride services reshape urban transportation systems, human mobility, and travelers' mode choice behavior. Compared to the traditional street-hailing taxi, an on-demand ride services platform analyzes ride requests of passengers and coordinates real-time supply and demand with dynamic operational strategies in the ride-sourcing market. To test the impact of dynamic optimization strategies on the ride-sourcing market, this paper proposes a dynamic vacant car-passenger meeting model. In this model, the accumulative arrival rate and departure rate of passengers and vacant cars determine the waiting number of passengers and vacant cars, while the waiting number of passengers and vacant cars in turn influence the meeting rate (which equals to the departure rate of both passengers and vacant cars). The departure rate means the rate at which passengers and vacant cars match up and start a paid trip. Compared with classic equilibrium models, this model can be utilized to characterize the influence of short-term variances and disturbances of current demand and supply (i.e., arrival rates of passengers and vacant cars) on the waiting numbers of passengers and vacant cars. Using the proposed meeting model, we optimize dynamic strategies under two objective functions, i.e., platform revenue maximization, and social welfare maximization, while the driver's profit is guaranteed above a certain level. We also propose an algorithm based on approximate dynamic programming (ADP) to solve the sequential dynamic optimization problem. The results show that our algorithm can effectively improve the objective function of the multi-period problem, compared with the myopic algorithm. A broader range of surge pricing and commission rate and the introduction of incentives are helpful to achieve better optimization results. The dynamic optimization strategies help the on-demand ride services platform efficiently adjust supply and demand resources and achieve specific optimization goals.

1. Introduction

In cities, taxi acts as an essential component of urban transportation systems due to its efficiency and flexibility. The strategies for regulating the taxi market have attracted researchers' interests since the 1970s. The early studies established

* Corresponding author.
E-mail address: cehyang@ust.hk (H. Yang).

https://doi.org/10.1016/j.trb.2020.05.005
0191-2615/

an aggregate supply-demand model to characterize the taxi's and passengers' behavior under the assumption of either a competitive or monopolistic market (Douglas, 1972; Beesley and Glaister, 1983; Cairns and Liston-Heyes, 1996). To capture the spatial structure in the meeting between a waiting customer and a vacant taxi, Yang and Wong (1998) first modeled urban taxi services at a network level. In that model with various origin-destination (OD) pairs, taxis chose one origin to pick up passengers by minimizing the cost of searching time. Based on the analytic framework, extended studies further characterize congestion effects, multiple taxi user classes and taxi modes, taxi's cruising strategies, and search frictions in the taxi market (Wong and Yang, 1998; Yang et al., 2001, 2005, 2010b, 2012, 2014; Ke et al., 2019; Yang and Yang, 2011).

The taxi market is a typical two-sided market with a platform (taxi company or the government) that connects the demand side (i.e., passengers) and supply side (i.e., vacant taxis). Passengers choose taxi services or other travel modes by considering the waiting time and taxi fare, while taxis decide locations to meet passengers by considering the trade-off between the profitability of the locations and searching costs to the locations. Yang and Yang (2011) first proposed a meeting function to characterize search frictions between drivers of vacant taxis and waiting passengers. It was pointed out that the meeting rate in one specific zone was determined by the density of waiting passengers and vacant taxis at that moment. The equilibrium state could be reached when the arrival rate of waiting passengers exactly matched the arrival rate of vacant taxis. There are two main leverages for the platform, i.e., price control, and entry limitation (which controls the taxi fleet size), to affect the equilibrium state of the taxi market.

The e-platform of on-demand ride services, which is enabled with emerging mobile internet techniques, is now reshaping the traditional taxi market. Although the on-demand ride services platform is similar to a taxi operator on providing a two-sided market, there exist differences between them. The on-demand ride services platform collects real-time information from both hailing cars and passengers, and thus has more leverages to influence the short-term demand and supply of the market. On the demand side, time-varying surge pricing (different charges during different time periods) implemented by the platform can affect passengers' willingness to select the travel mode of the on-demand ride services platform. On the supply side, the platform uses time-varying surge pricing, commission rate of trip fare, dispatching rules, and incentive mechanism (e.g., order bonus, point award, and dispatching priority) to determine the number of vacant cars during each time interval of a day. Also, some platforms (e.g., Uber, and DiDi) dispatch orders to the vacant hailing cars but do not let them independently select orders. It indicates that the models which characterize customer-search behavior of taxi can no longer represent the dispatch-oriented ride-sourcing market.

Since the emergence of on-demand ride services at the beginning of the 2010s, there have been extensive studies on analyzing drivers' and passengers' behavior in the ride-sourcing market. Zha et al. (2016) utilized the meeting function to characterize matching properties of the ride-sourcing market and examined the optimal pricing and fleet sizing strategies of the platform under a competitive and monopolistic market. He and Shen (2015) and Wang et al. (2016) examined drivers' and passengers' behavior in the e-hailing taxi market under the view of aggregated equilibrium and spatial equilibrium, respectively. Zha et al. (2017) modeled the labor supply of ride-sourcing drivers and investigated the impact of surge pricing using a bi-level optimization framework. The lower-level optimization model was used to capture the drivers' choices of working hours under an equilibrium state, while the upper-level optimization model was utilized to maximize the total revenue through surge pricing, i.e., differentiated pricing across hours. Yang et al. (2020b) developed a reward scheme integrated with surge pricing, which allowed users to pay an additional amount to a reward account during peak hours, and then use the balance in the reward account to compensate for their trips during off-peak hours.

Fruitful research efforts have been made to examine the ride-sourcing market and taxi market under the view of equilibrium, while how to characterize dynamic variances and cumulative effects of drivers' and passengers' numbers in multiple periods is still challenging. The assumption of equilibrium may not be reached when we consider a short time interval (such as several minutes), which limits its ability to capture short-term or real-time properties of different stakeholders of on-demand ride services.

In this paper, we make an initial attempt to utilize a meeting model to characterize the vacant car-passenger dynamic matching properties in a ride-sourcing market. In this model, the numbers of passengers and vacant cars are determined by the accumulative arrival/departure rate of passengers and vacant cars, respectively. We assume that the cumulative number of passengers and vacant cars in one day are equal rather than assuming equilibrium in each time instant or time interval, which is different from the previous studies. By further assuming the departure rates of vacant cars and passengers are equal to the meeting rate, the variables (including numbers of waiting vacant cars and passengers, and arrival rates of vacant cars and passengers) in the model are endogenously correlated. When the matching is executed at the end of each matching interval, the number of successful pairings depends on the numbers of passengers and vacant taxis in the two matching pools, and is independent of the detailed arrival process of passengers and vehicles within each short matching interval. It is not a microscopic bilateral searching and matching process as in the traditional cruising taxi markets, although drivers may strategically move to some locations. Both the potential vacant car supply rate and potential passenger demand rate are considered as exogenous variables in the model. Compared with classic equilibrium models, the endogenous variables in this dynamic meeting model is more sensitive to the current exogenous information (i.e., potential vacant car supply rate and potential passenger demand rate). Therefore, this proposed meeting model can be utilized to characterize the impact of short-term variances and disturbances of current demand and supply on the numbers of waiting passengers and vacant cars.

In the application process of the actual on-demand ride service platform, the operation problem is a classical dynamic programming multi-period optimization problem, which is usually solved by recursively computing. However, due to the

continuity of the state variables, exogenous variables, and decision variables, this problem suffers from the curse of dimensionality and becomes extremely hard to solve. So, we develop an effective non-myopic algorithm based on approximate dynamic programming (ADP) to solve it, in which we consider the real-time market's supply and demand information, as well as the influence of current operations on the following time periods, in the optimization process. The results show that ADP can effectively improve the objective function of the multi-period optimization model, compared to the myopic optimization algorithm. When a vast amount of demand (e.g., as a result of a special event) occurs, ADP is also able to significantly improve the effect of dynamic pricing and balance demand and supply.

Based on the proposed meeting model and ADP algorithm, we further test different operational strategies for different goals, e.g., platform revenue, and social welfare. We find that maximizing a certain objective function will cause different influences on other optimization goals. Finally, we test the sensitivity of optimization constraints, i.e., the range of surge pricing, bounds of commission rate, and the introduction of incentives for passengers/drivers, on different objective functions. The methodological contributions of this paper are threefold: (a) A dynamic vacant car-passenger meeting model is firstly proposed to characterize the current demand and supply's impact on the ride-sourcing market. (b) We simultaneously consider surge pricing, commission rate, and incentives for passengers/drivers, which is closer to the actual situation of the on-demand ride services platform's optimization strategies. (c) An ADP based algorithm is developed to solve the sequential decision problem.

The remainder of this paper is organized as follows. Section 2 presents a brief literature review on taxi market modeling, operations, and solution methodologies under the view of equilibrium, as well as some emerging studies on the on-demand ride services market. Section 3 proposes the dynamic vacant car-passenger meeting model and introduces platform operations such as surge pricing, commission rate, and incentives. The demand and supply based on the dynamic meeting scenario are discussed in Section 4. In Section 5, we formulate two platform objective functions and the corresponding optimization problems, then the solution algorithm based on ADP is developed. Section 6 presents the numerical experiments that examine the performance of the proposed model. Finally, Section 7 draws conclusions and outlooks on future research.

2. Literature review

The traditional taxi market has been extensively studied since the 1970s. The main difference between the taxi market and classical supply-demand market is that there always exist vacant taxis which cruise to pick up passengers, due to the spatial search frictions. Therefore, the total supplied service hour is always longer than the total demanded service hour. The gap between them determines the waiting time of passengers. In turn, both the passenger waiting time and taxi fare influence taxi demand, which results in a complicated and endogenous relationship between state variables in the taxi market. Under such an aggregated and abstract equilibrium framework, continuous efforts have been made by economists to better understand drivers' and passengers' behavior (Douglas, 1972; Beesley, 1973; De Vany, 1975).

In the 1990s, Yang and Wong (1998) modeled the spatial structure in equilibrium models and tried to understand taxi spatial customer-search behavior better. Since 2010, meeting functions had been utilized to model searching and meeting frictions between passengers and vacant taxis (Yang and Yang, 2011; Yang et al., 2012, 2014). A meeting function formulates the relationship between the meeting rate and numbers of vacant taxis and waiting passengers. The meeting rate is always monotonically increasing with the number of vacant taxis and waiting passengers, but the meeting function can exhibit increasing, constant, or decreasing returns to scale. Yang et al. (2010a) found that drivers may waste substantial time waiting in the airports, leading to a supply shortage in the downtowns, but further showed that a nonlinear fare structure could help alleviate this market failure. Chen et al. (2019) developed a physical model to capture passenger-driver matching process, then Zhang et al. (2019) tried to calibrate the parameters in the meeting functions based on the proposed physical model.

Recently, on-demand ride services platforms, e.g., Uber and DiDi, have changed the traditional taxi industry from the perspectives of the matching process and the supply side of the market. At the same time, they bring lots of interesting and challenging issues. Ride-sourcing or transportation network companies (TNCs) refer to an emerging urban mobility service mode in which private car owners use their own vehicles to provide for-hire rides (Chen et al., 2017). Ride-sourcing services can be completed via smartphone applications. The platform serves as a coordinator who matches requesting orders from passengers (demand) and vacant registered cars (supply). Consequently, the platform can adopt time-varying strategies to operate the meeting market, such as incentive mechanisms and surge pricing. For example, Yang et al. (2020a) proposed to dynamically adjust two key decision variables in the on-demand matching, namely, the matching time interval and matching radius, to maximize the system efficiency, in response to the real-time supply-demand conditions. Qian et al. (2017) investigated the taxi group ride problem that aimed at grouping passengers with a similar origin, destination, and departure time to save combinable trips, and explored the best incentives for a taxi group ride to maximize efficiency. According to that work, over 47% of the total taxi trip mileage might be saved by using the proper level of incentives. Surge pricing serves as one of the most common strategies of the on-demand ride services platform. It was proved that the platform which dynamically determined the price (for passengers) and wage (for drivers) could achieve a higher revenue than the platform providing the fixed commission (Cachon et al., 2017). Banerjee et al. (2015) proposed dynamic pricing strategies where the price was adjusted by the number of vacant cars in the queue. It was stated that the scheme of surge pricing performed better than the optimal static pricing when the platform didn't have complete information. Guda and Subramanian (2019) pointed out that the platform should adopt different strategies to manage the market based on the level of demand surge and the proportion of drivers needed to move from adjacent areas, such as informing drivers where to

move, incentives, and strategic surge pricing. Inspired by UberPool, Yan et al. (2019) discussed how to coordinate dynamic pricing and pool-matching technologies to better operate the ridepooling services, which allow one vehicle to serve two or more passengers in each ride. Bai et al. (2019) built an analytical model with endogenous supply and demand based on a queueing model and analyzed the optimal price/wage rates to optimize social welfare or platform revenue.

Most above works discuss the incentive mechanisms and surge pricing under the view of the taxi/ride-sourcing market's equilibrium. However, the ideal operating strategies of the ride-sourcing market should be time-varying based on real-time demand/supply information, which means that the strategies may change over time. Also, the market may not reach a stationary market equilibrium at every moment. So this paper introduces a dynamic vacant car-passenger meeting process to characterize the short-term variances and disturbances of demand and supply caused by the dynamic optimization strategies. At the same time, most of the previous studies concentrate on one specific kind of optimization strategies. By contrast, our paper integrates various optimization strategies (i.e., surge pricing, commission rate, and incentives) in a dynamic environment.

However, the dynamic optimization problem will become too complicated to solve if considering multiple optimization windows. To solve such sequential decision problems, the ADP algorithm is widely adopted to help dynamic programming overcome the challenge caused by three curses of dimensionality, i.e., state space, outcome space, and action space. The basic idea of the ADP algorithm is using some simulation and approximation methods to estimate the value function of a high-dimensional state space, and making decisions based on the estimated approximate value function (Bertsekas and Tsitsiklis, 1995; Powell et al., 2001; Powell, 2014). There were also some other dynamic pricing models proposed to tackle the challenging issues in the operations of the traditional taxi market and intelligent urban parking, which were also solved by ADP (Lei and Ouyang, 2017; Qian and Ukkusuri, 2017; Lei et al., 2020).

3. Dynamic vacant car-passenger meeting

3.1. Dynamic meeting model

In this section, we establish a dynamic meeting model to characterize the vacant car-passenger meeting process in the on-demand ride services market and discretize the whole day into a discrete-time finite-horizon system (i.e., K time intervals). The mathematical notations used in the paper are summarized in the appendix. Assuming that every time interval's length is Δt, one day will be divided into $60 \times 24/\Delta t$ time intervals in the following discussion. Therefore, every time interval is denoted as $t = k \cdot \Delta t$, $k \in \{1, \ldots, K\}$. If the time interval is small enough, the differences between the discretized market and the real-world market can be neglected. At last, the market clearing is assumed to be reached at the end of each day while we do not enforce equilibrium at every short time interval.

There are two underlying assumptions of the dynamic meeting process. (a) During every time interval, the number of meeting passengers/drivers is determined by a meeting function of the number of waiting passengers and the number of vacant cars. (b) For every time interval, both the numbers of waiting passengers and vacant cars are endogenously determined under a certain pricing strategy. These two assumptions were widely used in the static modeling framework of taxi markets. Moreover, in the ride-sourcing market, a common practice in actual operations is the batch matching in which the platform accumulates a certain number of idle drivers and waiting passengers and then implements a bipartite matching between the accumulated drivers and passengers. In this setting, as the matching is executed at the end of each matching interval, the number of successful pairings really depends on the numbers of passengers and vacant cars in the two matching pools. As a result, these two assumptions are still deemed realistic.

The supply and demand in a city are commonly heterogeneous over space and time, thus unbalanced supply and demand should be considered in real-world operation strategies. For a specific region, we suppose the arrival rate of passengers at time interval t is Q_t, the arrival rate of vacant cars at time interval t is T_t^{vc}. N_t^p and N_t^{vc} are denoted as the waiting numbers of passengers and vacant cars at time t, respectively. The meeting rate m_t (assumed to be the departure rate of both passengers and vacant cars) at time t is a function M of N_t^p and N_t^{vc}, while they can be calculated by the accumulative sum of the difference between the arrival rates of passengers and vacant cars, i.e., Q_t, T_t^{vc}, and meeting rate (departure rate) m_t. The mathematical relationships among these variables can be expressed as Eqs. (1)–(3), and illustrated in Fig. 1.

Meeting function:

$$m_t = M\left(N_t^p, N_t^{vc}\right) \tag{1}$$

Passengers:

$$N_t^p = CQ_t - CM_t = \sum_{s=0}^{t/\Delta t} \left(Q_{s\cdot\Delta t} - m_{s\cdot\Delta t}\right)\Delta t \tag{2}$$

Vacant cars:

$$N_t^{vc} = CT_t^{vc} - CM_t = \sum_{s=0}^{t/\Delta t} \left(T_{s\cdot\Delta t}^{vc} - m_{s\cdot\Delta t}\right)\Delta t \tag{3}$$

where $t \in \{\Delta t, \ \ldots, K\Delta t\}$.

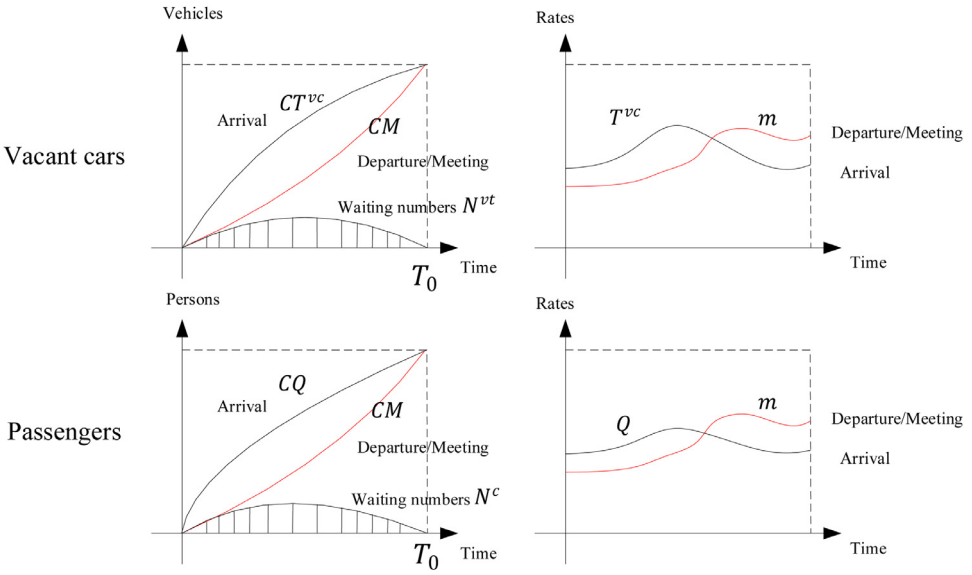

Fig. 1. An illustration of dynamic meeting.

For any time interval t, meeting rate m_t in Eq. (1) is nonnegative and continuously differentiable with $\partial m_t/\partial N_t^p > 0$ and $\partial m_t/\partial N_t^{vc} > 0$ in their domains $N_t^p \geq 0,\ N_t^{vc} \geq 0$. Furthermore, m_t approaches 0 as either N_t^p or N_t^{vc} is close to 0. As a result, we consider the following specific form of the Cobb-Douglas type production function (Varian, 2004) of vacant car-passenger meetings.

$$m_t = M\left(N_t^p, N_t^{vc}\right) = A\left(N_t^p\right)^{\alpha_1}\left(N_t^{vc}\right)^{\alpha_2} \tag{4}$$

where A is the meeting parameter, which is negatively related to the size of the searching and meeting area; α_1 and α_2 are the elasticities of the meeting rate with respect to the number of unserved customers and the number of vacant cars, respectively, at a given instant in time t. The Cobb-Douglas form meeting function is widely used in the modeling of taxi or ride-sourcing markets (e.g., Yang and Yang, 2011; Zha et al., 2016). Moreover, Yang et al. (2014) showed that the Cobb-Douglas form meeting function fits the relationships among passenger demand, average passenger waiting time and average taxi waiting and cruising time in search of each passenger well, evaluated with statistics in Hong Kong. They showed that the urban taxi services in Hong Kong exhibited a slight increasing return to scale.

While in a stationary equilibrium state with market clearing in any time (we assume $t \to \infty$ in that case), we have

$$\lim_{t\to\infty} Q_t = \lim_{t\to\infty} T_t^{vc} = \lim_{t\to\infty} m_t$$

3.2. Surge pricing, commission rate, and incentives

The pricing strategies of the on-demand ride services platform contain time-varying surge pricing, commission rate, and incentives for passengers/drivers. All of them can significantly affect the ride-sourcing market from different aspects. More specifically, time-varying surge pricing determines the passenger's trip fare and influence passenger's arrival rate. Vacant car's arrival rate is controlled by the driver's utility, which is related to time-varying surge pricing and the platform's commission rate. Further, both arrival rates of passengers and vacant cars are influenced by incentives for passengers/drivers.

While under the real on-demand ride services platform, these pricing strategies can be implemented by leveraging two variables (i.e., dynamic pricing multiplier λ_t and commission rate η_t). When $\lambda_t \geq 1$, λ_t corresponds to time-varying surge pricing, while λ_t represents the incentives for passengers when $\lambda_t < 1$. If η_t is positive, it means that the platform is leveraging the commission rate for drivers. When η_t changes from a positive value to a negative one, it will become an incentive for drivers. Therefore, these two variables (λ_t and η_t) are the main decision variables of the on-demand ride services platform, and the type of pricing strategy is determined by the specific values and bounds of the variables.

3.3. Relationship between variables

Under a certain pricing strategy, the relationship between various variables in the on-demand ride services market at time intervals is shown in Fig. 2, in which white, light, and dark boxes represent the decision variables, utility functions, and state variables, respectively. The impacts between different market variables take place along the solid lines. Given the certain exogenous information (i.e., the potential supply rate of vacant cars and potential demand rate of passengers),

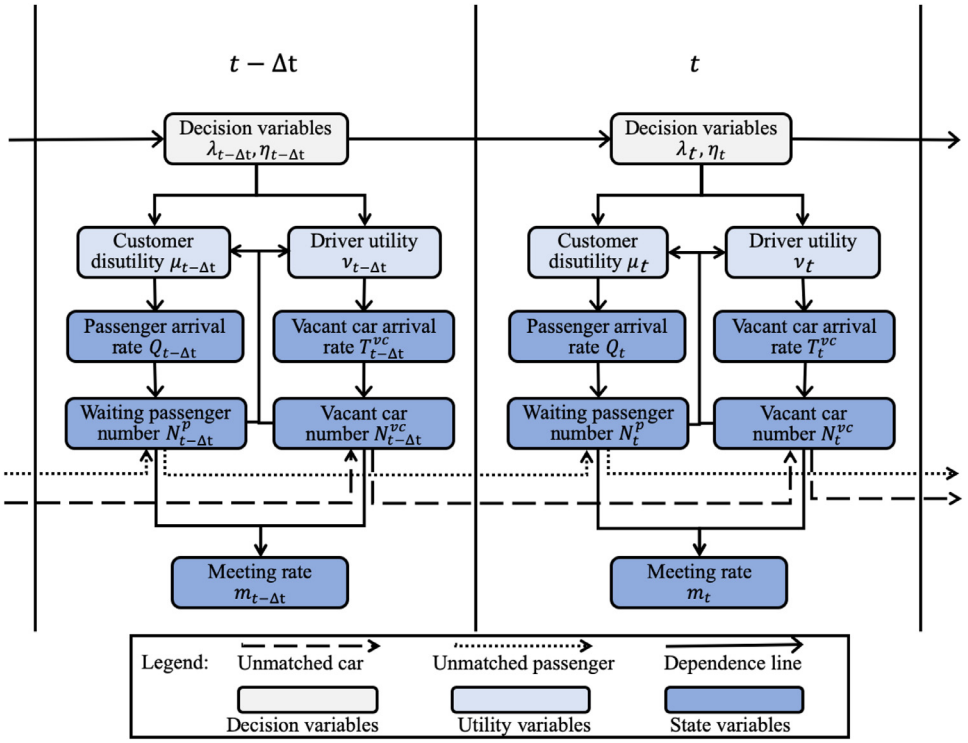

Fig. 2. Relationship between various market factors at different time intervals.

once the pricing strategy (i.e., dynamic pricing multiplier λ_t, and commission rate η_t) is determined, all utility and state variables in the market will be determined endogenously. On the demand side, potential customers will consider the trip fare (influenced by dynamic pricing multiplier) and waiting time for vacant cars. From the perspective of supply, potential drivers care about their income (influenced both by dynamic pricing multiplier and commission rate) and waiting time for passengers. Furthermore, combined with the exogenous variables, the utility variables will determine the arrival rate of passengers/vacant cars. Conversely, the number of waiting passengers and vacant cars will also influence the driver's utility and customer's disutility.

Finally, after the arrival rate and waiting number of passengers/vacant cars are determined endogenously, the meeting rate during every time interval can be obtained by the meeting function. The dashed lines and dotted lines represent remaining (unmatched) vacant cars and passengers in Fig. 2. As a result, given the pricing strategy and the exogenous information, all utility and state variables will be determined by the dynamic meeting market endogenously.

Since meeting rate m_t at different time intervals is determined by the aforementioned meeting function $M(N_t^c, N_t^{vt})$, m_t in discrete time intervals can be expressed as Eq. (5), and its relationship with λ_t, η_t can be written as $m(\lambda_t, \eta_t)$.

$$m_t = A\left(Q_t\Delta t + \sum_{s=0}^{t/\Delta t-1}(Q_{s\cdot\Delta t} - m_{s\cdot\Delta t})\Delta t\right)^{\alpha_1}\left(T_t^{vc}\Delta t + \sum_{s=0}^{t/\Delta t-1}\left(T_{s\cdot\Delta t}^{vc} - m_{s\cdot\Delta t}\right)\Delta t\right)^{\alpha_2} \tag{5}$$

4. Demand and supply

4.1. Passenger demand

In the on-demand ride-sourcing market, passenger's disutility μ_t is composed of the trip fare and monetary value of waiting time and travel time, given by

$$\mu_t = \overline{F_t} + \beta w_t^p + \beta_0 l_t \tag{6}$$

where $\overline{F_t} = F_o + \lambda_t F_t$ is the average trip fare; F_o is the flag-drop fee; λ_t is the dynamic pricing multiplier; $F_t = \omega l_t$ is the time-based charge; ω is the unit price of the average service time; l_t is the average passenger's trip time; w_t^p is the passenger waiting time; β is the monetary value of waiting time, and β_0 is the monetary value of in-vehicle travel time.

Inspired by Yang et al. (2010b), the meeting time in the market is $1/m_t$. Thus, the expected passenger waiting time w_t^p, which is proportional to the meeting time and the number of waiting passengers N_t^p, can be calculated by

$$w_t^p = \frac{N_t^p}{m_t} = \frac{1}{A\left(N_t^p\right)^{\alpha_1 - 1}\left(N_t^{vc}\right)^{\alpha_2}} \tag{7}$$

where A is the meeting parameter, α_1 and α_2 are the elasticities of the meeting rate in Eq. (4).

Passenger arrival rate Q_t at time t is determined by disutility μ_t, and demand function f should be a monotonically decreasing function on μ_t. Therefore, the demand function f is set as the following specific form:

$$Q_t = f(\mu_t) = \overline{Q_t}\ \exp(-\theta\mu_t) \tag{8}$$

where $\overline{Q_t}$ is the potential passenger demand rate; θ is the demand scaling parameter that indicates the sensitivity of demand to the full trip cost of passengers', and it can be calibrated from the observational data. The demand function (8) implicitly implies mode choices of passengers, who switch between ride-sourcing service and other modes; the demand for ride-sourcing service is given by Q_t, and the demand for other modes is given by $\overline{Q_t} - Q_t$. It is noteworthy that this representation of the demand function has been widely used in the literature (e.g., Yang et al., 2011; Zha et al., 2016).

The price elasticity of demand E_d based on function f is calculated in Eq. (9). It indicates that Q_t is relatively elastic, unit elastic, and relatively inelastic, if $\mu_t > \frac{1}{\theta}$, $\mu_t = \frac{1}{\theta}$, or $\mu_t < \frac{1}{\theta}$, respectively. This property of function f is used to describe that passenger demand is more sensitive to the disutility when the full trip price is relatively high and vice versa.

$$E_d = \frac{\partial Q_t}{\partial \mu_t}\frac{\mu_t}{Q_t} = -\theta\mu_t \tag{9}$$

Using the customer's disutility defined in Eq. (6) and the customer's waiting time function in Eq. (7), the passenger demand function can be written as

$$Q_t = \overline{Q_t}\ \exp\left[-\theta\left(F_o + \lambda_t F_t + \frac{\beta}{A\left(N_t^p\right)^{\alpha_1 - 1}\left(N_t^{vc}\right)^{\alpha_2}} + \beta_0 l_t\right)\right] \tag{10}$$

4.2. Supply and revenue

In the on-demand ride-sourcing market, we assume that every car driver is free to enter or exit the market. Therefore, they determine whether to work based on maximizing their expected utility v_t, which positively depends on expected revenue and negatively on waiting and in-service time (Wong et al., 2001). More specifically, the expected utility v_t is given by

$$v_t = \overline{F_t}(1 - \eta_t) - \phi\left(w_t^{vc} + l_t\right) \tag{11}$$

where $\overline{F_t}$ is average trip fare; η_t is the proportion that the platform extracts from the passenger fare; w_t^{vc} is vacant cars' waiting time; ϕ is the value of operating expense for one car.

In parallel to Eqs. (7), (12) states that the expected car waiting time is proportional to the meeting time and the number of waiting vacant cars N_t^{vc} (Yang et al., 2010b), given by

$$w_t^{vc} = \frac{N_t^{vc}}{m_t} = \frac{1}{A\left(N_t^p\right)^{\alpha_1}\left(N_t^{vc}\right)^{\alpha_2 - 1}} \tag{12}$$

The vacant car arrival rate T_t^{vc} at time t is determined by the car's utility v_t, and supply function g should be a monotonically increasing function on v_t when $v_t > \varepsilon_0$ (ε_0 is the opportunity cost of a driver). If driver utility v_t is less than ε_0, no car will enter the market. Therefore, the supply function g is set as the following specific form:

$$T_t^{vc} = g(v_t) = \begin{cases} \overline{T_t^{vc}} exp\left(-\frac{\delta}{v_t}\right), & v_t \geq \epsilon_0 \\ 0, & v_t < \epsilon_0 \end{cases} \tag{13}$$

where $\overline{T_t^{vc}}$ is the potential vacant car supply rate; δ is the supply scaling parameter that indicates the sensitivity of supply to the expected utility of drivers'.

The price elasticity of supply E_s based on function g is calculated in Eq. (14). It indicates that T_t^{vc} is relatively elastic, unit elastic, or relatively inelastic, if $v_t \langle \delta$, $v_t = \delta$, or $v_t \rangle \delta$, respectively. This property of function g is used to describe that car supply is more sensitive to the driver utility when the utility is relatively low and vice versa.

$$E_s = \frac{\partial T_t^{vc}}{\partial v_t}\frac{v_t}{T_t^{vc}} = \frac{\delta}{v_t} \tag{14}$$

Using the customer's trip fare, driver utility defined in Eq. (11) and vacant car's waiting time function of Eq. (12), the vacant car arrival function can be written as:

$$T_t^{vc} = g(v_t) = \begin{cases} \overline{T_t^{vc}} exp\left[-\frac{\delta}{(F_o + \lambda_t F_t)(1-\eta_t) - \phi\left(1/A\left(N_t^p\right)^{\alpha_1}\left(N_t^{vc}\right)^{\alpha_2 - 1} + l_t\right)}\right], & v_t \geq \epsilon_0 \\ 0, & v_t < \epsilon_0 \end{cases} \tag{15}$$

4.3. Market analysis

To simplify the analysis, we assume both α_1 and α_2 to be 1 in this subsection, and the sensitivity analysis of the market parameters will be numerically presented in Section 6. Firstly, we investigate the impact of commission rate η_t, and obtain Proposition 1.

Proposition 1. *With the increase of commission rate η_t, the numbers of passengers and drivers will both increase or decrease.*

Proof. We separately derive partial derivatives of the passenger's disutility μ_t and the driver's utility ν_t with respect to commission rate η_t to explore the impacts of η_t on market participants' utility or disutility. Recall Eqs. (4) (6)–(8), (11)–(13), we have

$$\frac{\partial \mu_t}{\partial \eta_t} = \frac{-\bar{F}_t \beta\delta \; T^{vc} \cdot \frac{\partial w_t^p}{\partial N_t^{vc}}}{\nu_t^2 - \phi\theta\beta\delta T_t^{vc} Q_t \cdot \frac{\partial w_t^p}{\partial N_t^{vc}} \frac{\partial w_t^{vc}}{\partial N_t^p}}$$

$$\frac{\partial \nu_t}{\partial \eta_t} = \frac{-\nu_t^2 \bar{F}_t}{\nu_t^2 - \phi\theta\beta\delta T_t^{vc} Q_t \cdot \frac{\partial w_t^p}{\partial N_t^{vc}} \frac{\partial w_t^{vc}}{\partial N_t^p}}$$

The denominators of the two partial derivatives are the same, but their numerators have opposite signs, because Eq. (7) indicates $\frac{\partial w_t^p}{\partial N_t^{vc}} < 0$. Therefore, one of the two partial derivatives is positive, while the other is negative. In one case, that is, $\frac{\partial \mu_t}{\partial \eta_t} > 0$ and $\frac{\partial \nu_t}{\partial \eta_t} < 0$, if commission rate η_t increases, then the passenger's disutility increases, while the driver's expected utility decreases. Thus, both numbers of passengers and drivers in the market will decrease. In the other case, that is, $\frac{\partial \mu_t}{\partial \eta_t} \langle 0$ and $\frac{\partial \nu_t}{\partial \eta_t} \rangle 0$, if commission rate η_t increases, then more passengers and drivers are willing to enter the market, and both of their numbers will increase. ■

Secondly, we investigate the impact of dynamic pricing multiplier λ_t, and obtain Proposition 2.

Proposition 2. –

Case 1. *Given $\frac{\partial \mu_t}{\partial \eta_t} > 0$ and $\frac{\partial \nu_t}{\partial \eta_t} < 0$, if $\frac{\partial \mu_t}{\partial \lambda_t} < 0$, then $\frac{\partial \nu_t}{\partial \lambda_t} > 0$, conversely, the relationship does not necessarily hold;*

Case 2. *Given $\frac{\partial \mu_t}{\partial \eta_t} < 0$ and $\frac{\partial \nu_t}{\partial \eta_t} > 0$, if $\frac{\partial \mu_t}{\partial \lambda_t} > 0$, then $\frac{\partial \nu_t}{\partial \lambda_t} < 0$, conversely, the relationship does not necessarily hold.*

Proof. Firstly, we separately derive the partial derivative of passenger's disutility μ_t and car driver's utility ν_t with respect to dynamic pricing multiplier λ_t to explore the impacts of λ_t on market participants' utility or disutility. Recall Eqs. (4, 6-8, 11-13), we have

$$\frac{\partial \mu_t}{\partial \lambda_t} = \frac{F_t\left[\nu_t^2 + (1-\eta_t)\beta\delta T_t^{vc} \cdot \frac{\partial w_t^p}{\partial N_t^{vc}}\right]}{\nu_t^2 - \phi\theta\beta\delta T_t^{vc} Q_t \cdot \frac{\partial w_t^p}{\partial N_t^{vc}} \frac{\partial w_t^{vc}}{\partial N_t^p}}$$

$$\frac{\partial \nu_t}{\partial \lambda_t} = \frac{F_t \nu_t^2\left(1 - \eta_t + \phi\theta Q_t \cdot \frac{\partial w_t^{vc}}{\partial N_t^p}\right)}{\nu_t^2 - \phi\theta\beta\delta T_t^{vc} Q_t \cdot \frac{\partial w_t^p}{\partial N_t^{vc}} \frac{\partial w_t^{vc}}{\partial N_t^p}}$$

Secondly, we prove Case 1 of Proposition 2. Given $\frac{\partial \mu_t}{\partial \eta_t} > 0$ and $\frac{\partial \nu_t}{\partial \eta_t} < 0$, we know that the denominator parts of those two partial derivatives are always negative based on the proof for Proposition 1. So $\nu_t^2 - \phi\theta\beta\delta T_t^{vc} Q_t \cdot \frac{\partial w_t^p}{\partial N_t^{vc}} \frac{\partial w_t^{vc}}{\partial N_t^p} > 0$, and it can be simplified into $1 + \beta\phi \frac{\partial Q_t}{\partial \mu_t} \frac{\partial T_t^{vc}}{\partial \nu_t} \frac{\partial w_t^p}{\partial N_t^{vc}} \frac{\partial w_t^{vc}}{\partial N_t^p} > 0$, further, we obtain $\frac{\partial \mu_t}{\partial Q_t} \frac{\partial \nu_t}{\partial T_t^{vc}} \frac{\partial N_t^{vc}}{\partial w_t^p} \frac{\partial N_t^p}{\partial w_t^{vc}} < -\beta\phi$. If $\frac{\partial \mu_t}{\partial \lambda_t} < 0$, then the numerator of $\frac{\partial \mu_t}{\partial \lambda_t}$ is negative, i.e., $\nu_t^2 + (1-\eta_t)\beta\delta T_t^{vc} \cdot \frac{\partial w_t^p}{\partial N_t^{vc}} < 0$. Since $\frac{\partial T_t^{vc}}{\partial \nu_t} = \frac{\delta T_t^{vc}}{\nu_t^2}$, we have $1 + (1-\eta_t)\beta \frac{\partial T_t^{vc}}{\partial \nu_t} \frac{\partial w_t^p}{\partial N_t^{vc}} < 0$, then $-\beta \frac{\partial T_t^{vc}}{\partial \nu_t} \frac{\partial w_t^p}{\partial N_t^{vc}} > \frac{1}{1-\eta_t}$. Given that $\frac{\partial \mu_t}{\partial Q_t} \frac{\partial \nu_t}{\partial T_t^{vc}} \frac{\partial N_t^{vc}}{\partial w_t^p} \frac{\partial N_t^p}{\partial w_t^{vc}} < -\beta\phi$, we have $\frac{\partial \mu_t}{\partial Q_t} \frac{\partial \nu_t}{\partial T_t^{vc}} \frac{\partial N_t^{vc}}{\partial w_t^p} \frac{\partial N_t^p}{\partial w_t^{vc}} \cdot \frac{\partial T_t^{vc}}{\partial \nu_t} \frac{\partial w_t^p}{\partial N_t^{vc}} > -\beta\phi \frac{\partial T_t^{vc}}{\partial \nu_t} \frac{\partial w_t^p}{\partial N_t^{vc}}$, so $\frac{\partial \mu_t}{\partial Q_t} \frac{\partial N_t^p}{\partial w_t^{vc}} > \phi(-\beta \frac{\partial T_t^{vc}}{\partial \nu_t} \frac{\partial w_t^p}{\partial N_t^{vc}}) > \frac{\phi}{1-\eta_t}$. We know that $\frac{\partial \mu_t}{\partial Q_t} \frac{\partial N_t^p}{\partial w_t^{vc}} > \frac{\phi}{1-\eta_t}$ can be reformulated as $1 - \eta_t - \phi \frac{\partial Q_t}{\partial \mu_t} \frac{\partial w_t^{vc}}{\partial N_t^p} > 0$. As a result, the numerator of $\frac{\partial \nu_t}{\partial \lambda_t}$ is positive, then $\frac{\partial \nu_t}{\partial \lambda_t} > 0$.

Finally, we prove Case 2 of Proposition 2. Following the same logic used to prove Case 1 of Proposition 2, given $\frac{\partial \mu_t}{\partial \eta_t} < 0$ and $\frac{\partial \nu_t}{\partial \eta_t} > 0$, we have $\frac{\partial \mu_t}{\partial Q_t} \frac{\partial \nu_t}{\partial T_t^{vc}} \frac{\partial N_t^{vc}}{\partial w_t^p} \frac{\partial N_t^p}{\partial w_t^{vc}} > -\beta\phi$. If $\frac{\partial \mu_t}{\partial \lambda_t} > 0$, then $\nu_t^2 + (1-\eta_t)\beta\delta T_t^{vc} \cdot \frac{\partial w_t^p}{\partial N_t^{vc}} > 0$. Therefore, $1 + (1-\eta_t)\beta \frac{\partial T_t^{vc}}{\partial \nu_t} \frac{\partial w_t^p}{\partial N_t^{vc}} > 0$, then $-\beta \frac{\partial T_t^{vc}}{\partial \nu_t} \frac{\partial w_t^p}{\partial N_t^{vc}} < \frac{1}{1-\eta_t}$. Since $\frac{\partial \mu_t}{\partial Q_t} \frac{\partial \nu_t}{\partial T_t^{vc}} \frac{\partial N_t^{vc}}{\partial w_t^p} \frac{\partial N_t^p}{\partial w_t^{vc}} > -\beta\phi$, we have $\frac{\partial \mu_t}{\partial Q_t} \frac{\partial \nu_t}{\partial T_t^{vc}} \frac{\partial N_t^{vc}}{\partial w_t^p} \frac{\partial N_t^p}{\partial w_t^{vc}} \cdot \frac{\partial T_t^{vc}}{\partial \nu_t} \frac{\partial w_t^p}{\partial N_t^{vc}} <$

$-\beta\phi\frac{\partial T_t^{vc}}{\partial v_t}\frac{\partial w_t^p}{\partial N_t^{vc}}$, thus, $\frac{\partial \mu_t}{\partial Q_t}\frac{\partial N_t^p}{\partial w_t^{vc}} < \phi(-\beta\frac{\partial T_t^{vc}}{\partial v_t}\frac{\partial w_t^p}{\partial N_t^{vc}}) < \frac{\phi}{1-\eta_t}$. We know that $\frac{\partial \mu_t}{\partial Q_t}\frac{\partial N_t^p}{\partial w_t^{vc}} < \frac{\phi}{1-\eta_t}$ can be reformulated as $1-\eta_t-\phi\frac{\partial Q_t}{\partial \mu_t}\frac{\partial w_t^{vc}}{\partial N_t^p} < 0$. As a result, the numerator of $\frac{\partial v_t}{\partial \lambda_t}$ is negative, then $\frac{\partial v_t}{\partial \lambda_t} < 0$. ■

These conclusions have practical value for the on-demand ride services platform. Proposition 1 implies that the numbers of passengers and drivers will both increase or decrease under a higher commission rate η_t. Intuitively, fewer passengers and drivers are willing to participate in the market when commission rate η_t increases. As a result, Case 1 in Proposition 2 is more common for most cases in the real world. The conclusion, if $\frac{\partial \mu_t}{\partial \lambda_t} < 0$, then $\frac{\partial v_t}{\partial \lambda_t} > 0$, is equivalent with that if $\frac{\partial v_t}{\partial \lambda_t} < 0$, then $\frac{\partial \mu_t}{\partial \lambda_t} > 0$. These two findings are helpful when the platform aims to attract more passengers and drivers into the market only by leveraging its ride-sourcing service's price with a certain commission rate. On the one hand, if the platform considers increasing its service's price, it should pay more attention to passengers' willingness to use its platform. Because the more passengers are inclined to use the platform ($\frac{\partial \mu_t}{\partial \lambda_t} < 0$), the more drivers can be guaranteed to participate on the platform ($\frac{\partial v_t}{\partial \lambda_t} > 0$). On the other hand, if the platform considers decreasing its service's price, then it should focus on the drivers' willingness to provide services on it. This is because if the proportion of drivers who are willing to provide services on the platform increases ($\frac{\partial v_t}{\partial \lambda_t} < 0$), passengers will correspondingly increase their willingness to use the platform ($\frac{\partial \mu_t}{\partial \lambda_t} > 0$).

5. Optimization problem formulation

5.1. Objective functions

Given the dynamic and comprehensive supply/demand information, we can adjust the pricing strategies, i.e., decision variables, to achieve different specific goals. Although there could be several different objectives for the on-demand ride services market, different participants in the market will concentrate on different targets from their own perspectives. In this paper, we consider two different objectives, i.e., platform revenue maximization, and social welfare maximization, from the perspective of platform, and government regulators, respectively.

For the ride-sourcing platform, the most crucial target is to maximize the platform revenue, which is calculated by $R_t(\lambda_t,\ \eta_t) = \overline{F}_t m_t \eta_t$. In this case, the optimization problem for the platform is formulated as follows:

$$\max_{\boldsymbol{\lambda},\ \boldsymbol{\eta}} \sum_{s=0}^{K-1} R_{s\cdot\Delta t} \tag{16}$$

where vectors $\boldsymbol{\lambda}$ and $\boldsymbol{\eta}$ are two sequences of decision variables, i.e., $[\lambda_{\Delta t}, \ldots, \lambda_{(K-1)\cdot\Delta t}]$, and $[\eta_{\Delta t}, \ldots, \eta_{(K-1)\cdot\Delta t}]$.

Meanwhile, from the perspective of the government, it aims to maximize social welfare. Social welfare is the total benefit available to the society from an economic transaction, which can be defined by Eq. (17) in this dynamic meeting model.

$$SW_t(\lambda_t,\ \eta_t) = CS_t + PS_t + R_t - \beta\Delta t\left(N_t^p - m_t\right) - \phi\Delta t\left(N_t^{vc} - m_t\right)$$

where CS_t is the consumer surplus defined by $\int_0^{m_t} f^{-1}(z)\mathrm{d}z - \mu_t m_t$; PS_t is the producer surplus defined by $v_t m_t - \int_0^{m_t} g^{-1}(z)\mathrm{d}z$; $\beta\Delta t(N_t^p - m_t)$ is the value of waiting time for unmatched passengers from t to $t+\Delta t$; $\phi\Delta t(N_t^{vc} - m_t)$ is the value of waiting time for unmatched vacant cars from t to $t+\Delta t$.

The optimization problem for the platform to maximize social welfare is given by

$$\max_{\boldsymbol{\lambda},\ \boldsymbol{\eta}} \sum_{s=0}^{K-1} SW_{s\cdot\Delta t} \tag{17}$$

The relationship among consumer surplus, producer surplus, and platform revenue in a market-clearing market with equilibrium is illustrated in Fig. 3.

As mentioned before, the platform can leverage decision variables to achieve specific objectives. However, this process is not easy because the change of decision variables has very complicated impacts on the market. As commission rate η increases, the platform can get more money from a ride-sourcing order, which may elevate platform revenue. However, the driver utility will decrease. Further, the vacant car arrival rate decreases will lead to an increase in the passenger waiting time.

As a consequence, there will be fewer passengers due to the rise in the consumer disutility, which will let the number of ride-sourcing orders down and may lower platform revenue. In conclusion, when the platform aims to obtain more revenue by leveraging commission rate η, there is a trade-off between one ride-sourcing order's revenue and the number of ride-sourcing orders. This trade-off becomes more complicated under different demand and supply situations. Also, the change of dynamic pricing multiplier λ faces a similar trade-off issue. When we turn to the social welfare objective, the same difficulty still exists. Consequently, the best strategy for the platform is to adapt the decision variables based on real-time demand and supply situations.

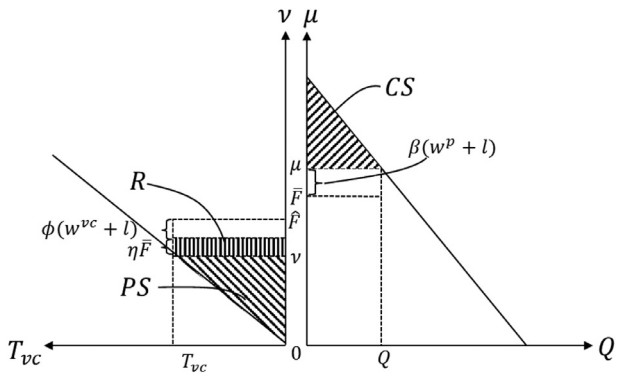

Fig. 3. An illustration of consumer surplus, producer surplus, and platform revenue in a market-clearing market with equilibrium.

5.2. Constraints

Given certain decision variables, all of the state variables of dynamic vacant car-passenger meeting at every time interval can be characterized by Eqs. (5), (10), and (15). Therefore, these three equations are set as constraints of the optimization problem. Also, another key participator of the market, i.e., drivers, mostly concern their income when they determine whether to participate in the market, which is calculated by the total income $\overline{F}_t m_t(1-\eta_t)$ divided by the arrival rate of drivers T_t^{vc} at time interval t. Thus, drivers' profit should be guaranteed above a certain level. Furthermore, this acquirement can be written as the following constraint:

$$\frac{\overline{F}_t m_t(1-\eta_t)}{T_t^{vc}} \geq c, \ \forall t \tag{18}$$

where c is the minimum wage rate for drivers.

As shown in Fig. 2, there are only two decision variables, i.e., dynamic pricing multiplier λ_t, and platform commission rate η_t. When the platform leverages decision variables to achieve specific goals, the range of variables can be effectively adapted to different operational scenarios. In other words, λ_t corresponds to time-varying surge pricing when $\lambda_t \geq 1$ or incentives for passengers when $\lambda_t < 1$; positive η_t corresponds to the commission rate for drivers, while negative η_t corresponds to incentives for drivers.

Considering the actual application, the fluctuation of decision variables should not be too frequent or intense. It is worth to mention that, in actual operations, the platforms may restrict the fluctuation of surge pricing and wage. This is because frequently changing the price and wage may make passengers and drivers uncomfortable. For example, when a passenger opens the APP, the price shows \$5, then when she/he presses the button to request an order, the price becomes \$10, then the passenger may be annoyed. Hence, we impose constraints (19)-(23) as the restriction over pricing strategies. Constraint (19) states that the pricing decision variables only change every n time interval length (one decision epoch). That is, one day will be divided into $\frac{K}{n}$ decision epochs, and the decision variables should be constants in one decision epoch. Constraints (20)–(21) restrict the fluctuation of dynamic pricing multiplier λ_t and platform commission rate η_t between two consecutive decision epochs within the range of $[-\varepsilon_1, \varepsilon_2]$, and $[-\varepsilon_3, \varepsilon_4]$, respectively. In addition, pricing decision variables are often subject to certain restrictions enforced by city legislators in practice; therefore, we use constraints (22)–(23) to enforce two lower limits λ^L, η^L and two upper limits λ^U, η^U, respectively.

$$\begin{cases} \lambda_{k\cdot\Delta t} = \lambda(j) \\ \eta_{k\cdot\Delta t} = \eta(j) \end{cases} \text{ if } (j-1)\cdot n + 1 \leq k \leq j\cdot n, j \in \left\{1, \ \ldots, \frac{K}{n}\right\} \tag{19}$$

$$-\epsilon_1 \leq \lambda(j) - \lambda(j-1) \leq \epsilon_2, \ \forall j \in \left\{1, \ldots, \frac{K}{n}\right\} \tag{20}$$

$$-\epsilon_3 \leq \eta(j) - \eta(j-1) \leq \epsilon_4, \ \forall j \in \left\{1, \ \ldots, \frac{K}{n}\right\} \tag{21}$$

$$\lambda^L \leq \lambda(j) \leq \lambda^U, \ \forall j \in \left\{1, \ \ldots, \frac{K}{n}\right\} \tag{22}$$

$$\eta^L \leq \eta(j) \leq \eta^U, \ \forall j \in \left\{1, \ \ldots, \frac{K}{n}\right\} \tag{23}$$

In conclusion, we summarize constraints (5), (10), (15), and (18)–(23) for the optimization problem.

5.3. Solution algorithm

The two optimization problems formulated in Section 5.1 and Section 5.2 are all sequential decision problems, which means we can adopt a myopic optimization algorithm to solve them. For example, in this section, we try to maximize the whole days' platform revenue, and the optimization problem is shown in Eq. (24). During every decision epoch, the myopic optimization problem is to maximize the total platform revenue of the current decision epoch. Take one decision epoch $(t + \Delta t,\ t + n\Delta t)$ as an example, the objective function is the summation of platform revenue of n time intervals, expressed by Eq. (24). Since it is a finite time window problem, we can solve it by some traditional optimization algorithms, such as the sequential least squares programming algorithm (SLSQP).

$$\max_{\lambda_{t+\Delta t}\dots\lambda_{t+n\Delta t},\ \ \eta_{t+\Delta t}\dots\eta_{t+n\Delta t}} \sum_{s=0}^{n-1} R_{(t+s\cdot\Delta t)} \tag{24}$$

For the non-myopic optimization problem, objective function (24) can be rewritten as (25) by using the notation of dynamic programming. C_t is the one-stage objective function and equals $\sum_{s=0}^{n-1} R_s(\lambda_{t+s\cdot\Delta t},\ \eta_{t+s\cdot\Delta t})$. The state variables in every decision epoch are remaining vacant cars N_t^{vc} and passengers N_t^p in the last time segment, and the exogenous information includes the potential passenger demand rate and potential car supply rate. The state transition function is shown as follows:

$$\max_{\boldsymbol{\lambda},\ \boldsymbol{\eta}} \sum_{i=0}^{K/n-1} C_{i\cdot n\cdot\Delta t} \tag{25}$$

$$N_{t+n\cdot\Delta t}^{vc} = N_t^{vc} + \sum_{s=1}^{n} \left(T_{t+s\cdot\Delta t}^{vc} - m_{t+s\cdot\Delta t}\right)\Delta t \tag{26}$$

$$N_{t+n\cdot\Delta t}^{p} = N_t^{p} + \sum_{s=1}^{n} \left(Q_{t+s\cdot\Delta t} - m_{t+s\cdot\Delta t}\right)\Delta t \tag{27}$$

This problem seems to be solvable at first glance because we can solve the problem by recursively computing the following Bellman's optimality equation.

$$V_t\left(N_t^p, N_t^{vc}\right) = \max_{\lambda_{t+\Delta t}\dots\lambda_{t+n\cdot\Delta t},\ \ \eta_{t+\Delta t}\dots\eta_{t+n\cdot\Delta t}} \left\{C_t + E\left\{V_{t+n\cdot\Delta t}\left(N_{t+n\cdot\Delta t}^p, N_{t+n\cdot\Delta t}^{vc}\right)\right\}\right\} \tag{28}$$

where $V_t(N_t^p, N_t^{vc})$ is a value function that tells us the value of being in state (N_t^p, N_t^{vc}), calculated by the summation of the objective function C_t and the reward value function $V_{t+n\cdot\Delta t}(N_{t+n\cdot\Delta t}^p, N_{t+n\cdot\Delta t}^{vc})$ of subsequent time segments.

Nevertheless, the multi-period optimization problem's state, exogeneity, and decision spaces may scale exponentially over time due to the curse of dimensionality. Especially, some extreme states may occur in the real-world market. Therefore, we cannot guarantee that the infinite sample paths over time are all attempted, and every possible state is visited to obtain the best solution. Alternatively, we adopt the ADP algorithm to solve the problem, in which we use a suitably designed value function approximation (VFA) $\bar{V}_t(N_t^p, N_t^{vc})$ to approximate the future impact of the state (N_t^p, N_t^{vc}). Inspired by Lei and Ouyang (2017), the VFA of this paper is designed as a separable piecewise linear function of state variables. The piecewise linear function can provide a more stable approximation than a purely linear function and can be easily embedded into an optimization model with a maximization objective that is solvable by existing solvers. More specifically, for each time interval t, we use the summation of a set of one-dimensional functions $\bar{V}_{t,\ N_t^p}(N_t^p)$ and $\bar{V}_{t,\ N_t^{vc}}(N_t^{vc})$ to approximate $V_t(N_t^p, N_t^{vc})$, where $\bar{V}_{t,\ N_t^p}(N_t^p)$ and $\bar{V}_{t,\ N_t^{vc}}(N_t^{vc})$ are the piecewise linear functions of N_t^p and N_t^{vc}, respectively. These two functions are only related to one of the two state variables separately as follows:

$$\bar{V}_t\left(N_t^p, N_t^{vc}\right) = \bar{V}_{t,\ N_t^p}\left(N_t^p\right) + \bar{V}_{t,\ N_t^{vc}}\left(N_t^{vc}\right) \tag{29}$$

To train the parameters of piecewise linear functions in the VFA, we simulate different states with the forwarding time order and solve the following one-stage problem (34), where $\bar{V}_{t+n\cdot\Delta t}^{n-1}$ is the latest VFA. By calculating the marginal value information of state variables $\hat{\boldsymbol{v}}_t^n$ (i.e., the gradient of state variables at iteration n), we update the VFA parameters in different decision epochs with n iterations.

$$\max_{\lambda_{t+\Delta t}\dots\lambda_{t+n\cdot\Delta t},\ \ \eta_{t+\Delta t}\dots\eta_{t+n\cdot\Delta t}} \left\{C_t + \bar{V}_{t+n\cdot\Delta t}^{n-1}\left(N_{t+n\cdot\Delta t}^p, N_{t+n\cdot\Delta t}^{vc}\right)\right\} \tag{30}$$

The VFA update process is designed as Eq. (31), $\alpha^n = 1 - 1/(2n + 2) \in (0, 1)$ is the step size and set to be ascending with the iteration time n to ensure a quick convergence. Noted that though Eq. (31) only updates the VFA value with the current simulation status, the whole VFA will also automatically adapt to the updated value to ensure the continuity of the piecewise linear function in the update process. The iteration algorithm used to update its VFA coefficients is illustrated in Algorithm 1.

$$\bar{V}_t^n\left(N_t^p, N_t^{vc}\right) = \begin{cases} \alpha^{n-1}\cdot\bar{V}_t^{n-1}\left(N_t^p, N_t^{vc}\right) + \left(1-\alpha^{n-1}\right)\cdot\hat{\boldsymbol{v}}_t^n, & \textit{for current simulation status} \\ \bar{V}_t^{n-1}\left(N_t^p, N_t^{vc}\right), & \textit{for other status} \end{cases} \tag{31}$$

Algorithm 1 ADP algorithm

```
Set n = 0, ∀t, initialize VFA V̄_t^0(N_t^p, N_t^vc).
For n = 0 to N do
  Sample endogenous variables Q_t and T_t^vc for t = Δt to KΔt.
  For t = Δt, nΔt, 2nΔt....., KΔt do
    Solve simulation-based one-stage problem (30) using the latest VFA V̄_t^{n-1}.
    Calculate the gradient v̂_t^n at iteration n.
    Update VFA V̄_t^n(N_t^p, N_t^vc) based on Eq. (31).
  End for
  State transition using Eqs. (26-27).
End for
Output V̄_t^N(N_t^p, N_t^vc), ∀t
```

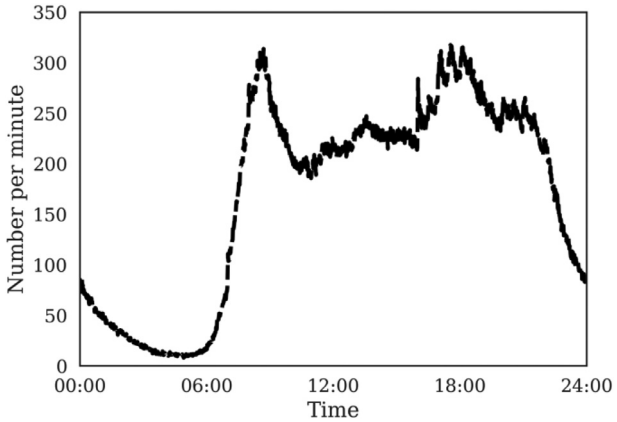

Fig. 4. Matched orders per minute in Hangzhou, China (two-week mean).

6. Numerical study

In this section, we use real-world ride-sourcing order data from DiDi Chuxing in Hangzhou, China. The data were collected in two weeks. The number of meeting passengers/vacant cars per minute is shown in Fig. 4, in which the number of matched orders during the extended morning peak (07:00-11:00) and evening peak (17:00-22:00) is significantly larger than other time periods.

6.1. Calibration of market parameters

To estimate the actual potential supply and demand in the ride-sourcing market, we assume that both the potential passenger demand rate $\overline{Q_t}$ and potential car supply rate $\overline{T_t^{vc}}$ are proportional to the real-world average rates of passengers and vacant cars at time t, respectively. After determining the numbers of potential passengers and cars, there are several market parameters to be calibrated, i.e., meeting parameter A, α_1 and α_2 in the meeting function, flag-drop fee F_0, price of average service time ω, average passenger's trip time l_t, monetary value of passenger's waiting time β and in-vehicle travel time β_0, demand scaling parameter θ, value of operating expense for one car φ, and supply scaling parameter δ. To simplify the calculation, we calibrate them with the following values based on the real-world situation. The market parameter setting and calibration results are summarized in Table 1.

To verify the plausibility of our calibration results, we analyze the characteristics of the market under fixed price and compare it with the real market data where there is no dynamic pricing and with a 20% commission rate. Fig. 5 shows the time-varying meeting numbers per minute in the real-world market and simulated market with calibrated parameters. The normalized root mean square error (NRMSE) and R-squared of two curves are 5.39% and 0.994, respectively, which indicate that there is no significant difference between them. Therefore, we believe that the two markets share the same characteristics in terms of the aforementioned meeting passengers or vacant cars. Furthermore, several state variables in the simulated scenario are shown in Fig. 6, i.e., number of waiting passengers, number of vacant cars, and meeting number. We capture some market characteristics that can be observed in the real-world market. For example, the number of waiting passengers is significantly higher than that of vacant cars in the morning and evening peaks, while there are more vacant cars than waiting passengers during the remaining time periods. It should be mentioned that the meeting number per minute is much smaller than those of waiting passengers and vacant cars, because they will keep waiting for several minutes until being matched or leaving the market. In summary, the simulated market can adequately reflect the characteristics of

Table 1
Market parameter setting and calibration

Parameter	Value	Unit	Source
A	10	-	Estimated in this paper
c	2	RMB	Parameter setting of this paper
F_o	10	RMB	DiDi in Hangzhou, China
l_t	0.3	h	DiDi in Hangzhou, China
Δt	1	min	Parameter setting of this paper
α_1	0.55	-	Assumed in this paper, and inspired by Yang et al. (2014) and Shao et al. (2016)
α_2	0.55	-	Assumed in this paper, and inspired by Yang et al. (2014) and Shao et al. (2016)
β	30	RMB/h	Referred to local average income level in Hangzhou, China
β_0	30	RMB/h	Referred to local average income level in Hangzhou, China
δ	30	RMB	Estimated in this paper
θ	0.04	1/RMB	Estimated in this paper
φ	60	RMB/h	DiDi in Hangzhou, China
ω	140	RMB/h	DiDi in Hangzhou, China

Note: - not applicable; RMB 100 = USD 14.4.

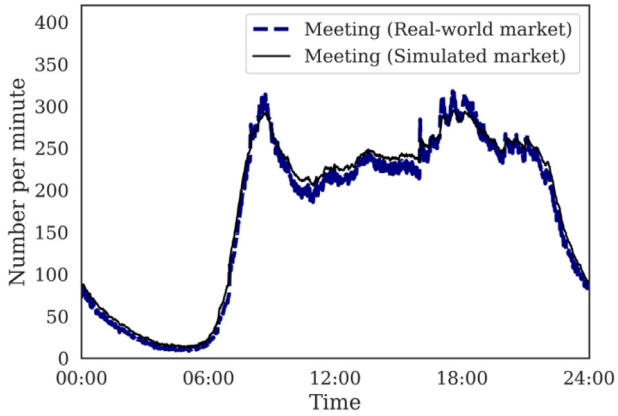

Fig. 5. Comparison of meeting numbers per minute between the real-world market and simulated market.

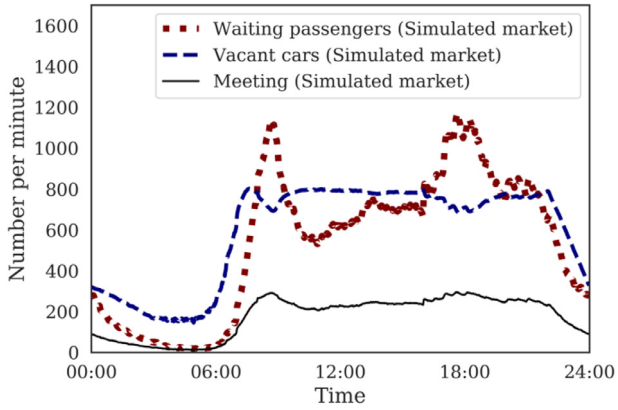

Fig. 6. State variables in the simulated market.

the real-world market, and if there is no specific reference, the mentioned market refers to the simulated market based on our dynamic vacant car-passenger meeting model in the following.

After the calibration of the market parameters, we separately adjust dynamic pricing multiplier λ and platform commission rate η to simulate different fixed-price strategies. Fig. 7 shows that both social welfare and platform revenue of one day vary with λ, given a constant $\eta = 0.2$. It also illustrates that with the increase of λ, both social welfare and platform revenue rise first and then fall, which is consistent with the trade-off mentioned previously in Section 5.1. When the values of λ are around 0.9 and 1.1, social welfare and total revenue of one day reach their maximum, respectively, which indicates that there is an appropriate balance between one ride-sourcing order's revenue and the number of ride-sourcing orders. As

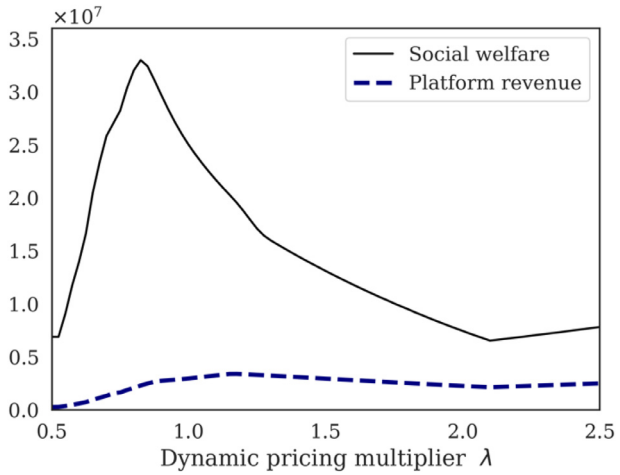

Fig. 7. Effect of dynamic pricing multiplier λ on different objective functions ($\eta = 0.2$)

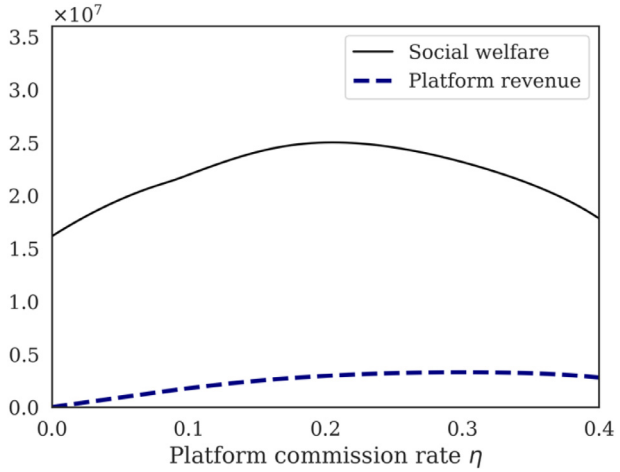

Fig. 8. Effect of platform commission rate η on different objective functions ($\lambda = 1$)

shown in Fig. 8, the social welfare and platform revenue also present a similar trend for the platform commission rate, and the platform revenue reaches its maximum when η is around 0.25 under $\lambda = 1$.

6.2. Comparison of different pricing strategies

To test the impacts of different pricing strategies on the market performance, we introduce a two-hour experiment from 15:00 to 17:00, the objective of which is to maximize social welfare in Eq. (17). In this experiment, one decision epoch is 15 min (i.e., $n = 15$) and the constraints of the optimization problem are set by $\varepsilon_1, \varepsilon_2 = 0.5,\ 0.5,\ \lambda^L, \lambda^U = 0.6,\ 1.4,\ \varepsilon_3, \varepsilon_4 = 0.2,\ 0.2,\ \eta^L, \eta^U = 0,\ 0.4$. Also, the experiment applies three pricing strategies, namely dynamic pricing based on the ADP algorithm, dynamic pricing based on the myopic algorithm, and fixed price. As shown in Fig. 9, the cumulative social welfare with dynamic pricing based on the myopic algorithm is 24.5% greater than that with a fixed price. Meanwhile, the objective function value obtained by the ADP algorithm increases by 26.2% compared with the result of the myopic algorithm. Based on the results, we can observe that dynamic pricing significantly increases social welfare, while the effect of the ADP algorithm is much better than the myopic algorithm. As shown in Fig. 9(a) and (b), the social welfare of dynamic pricing (ADP) is lower than that of dynamic pricing (myopic) in the first and third decision epochs. However, in the remaining decision epochs, social welfare with dynamic pricing (ADP) performs more steadily and catches up with the one with dynamic pricing (myopic) after 16:00. Apparently, at the end of the experiment, the objective function (i.e., cumulative social welfare) with dynamic pricing (ADP) is much better than that of dynamic pricing (myopic). This is because, in several decision epochs (e.g., the third epoch), the ADP algorithm values the state variables' impact on the future more than the current decision epoch's social welfare based on the latest VFA. After several repetitive experiments, we find that dynamic pricing can evidently improve the corresponding optimization objective function, and the ADP algorithm always performs better

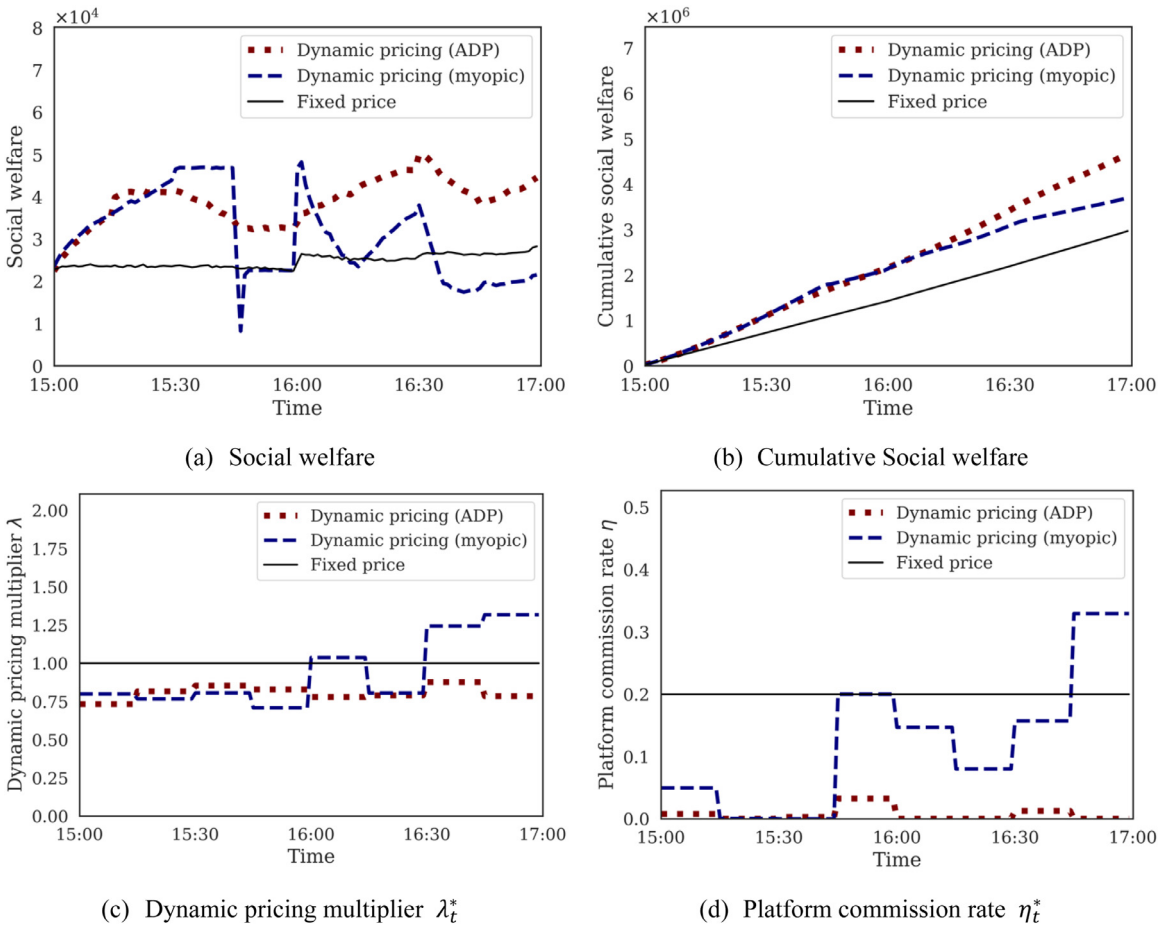

Fig. 9. Optimization results of the ADP dynamic pricing, myopic dynamic pricing, and fixed price (Objective: Social welfare).

than the myopic algorithm for objective functions (16) and (17), and the extent of increase depends on the demand/supply situation and selected objective functions. Therefore, we focus on the ADP algorithm to solve the multi-period optimization problem under dynamic pricing scenarios in the following experiments.

6.3. Analysis of different objective functions

This section studies the impacts of different objective functions under the dynamic pricing scenarios. The two scenarios with objective functions (16) and (17), i.e., platform revenue maximization and social welfare maximization, are separately considered in these experiments, and the constraints of the optimization problems remain the same as Section 6.2. The optimal results and corresponding decision variables obtained by the ADP algorithm are shown in Fig. 10, indicating the change of platform revenue and social welfare under two scenarios. Fig. 11 illustrates the decision variables under different dynamic optimization scenarios. The results show that the platform tends to raise dynamic pricing multiplier λ and platform commission rate η when it chooses to optimize platform revenue. Therefore, the platform revenue keeps higher in such circumstances. In contrast, social welfare under this scenario is worse than the other scenario. For this reason, although revenue maximization is the most beneficial strategy for commercial platforms, this strategy may be harmful to social welfare. If the objective function is set as social welfare, the platform will slightly reduce its price and keep η close to zero. As shown in Fig. 10(a), this strategy harms the platform revenue, which is far below the other scenario. The results also illustrate that only maximizing social welfare is not a sustainable development strategy for commercial platforms. This conclusion is reasonable due to the full flexibility of passengers and drivers, and consistent with previous research (e.g., Zha et al., 2016).

As shown in Fig. 12, the market with social welfare maximization generates a larger meeting number than the platform revenue maximization scenario, while it leads to a significant imbalance between supply and demand, as well as fluctuations in the number of waiting passengers in the market. This is because the platform reduces its price to maximize social welfare, which stimulates many passengers to use the ride-sourcing platform. Meanwhile, the lower price for the trips will cause drivers to be unwilling to provide services. However, due to the reduced platform commission rate and saved vacant cars'

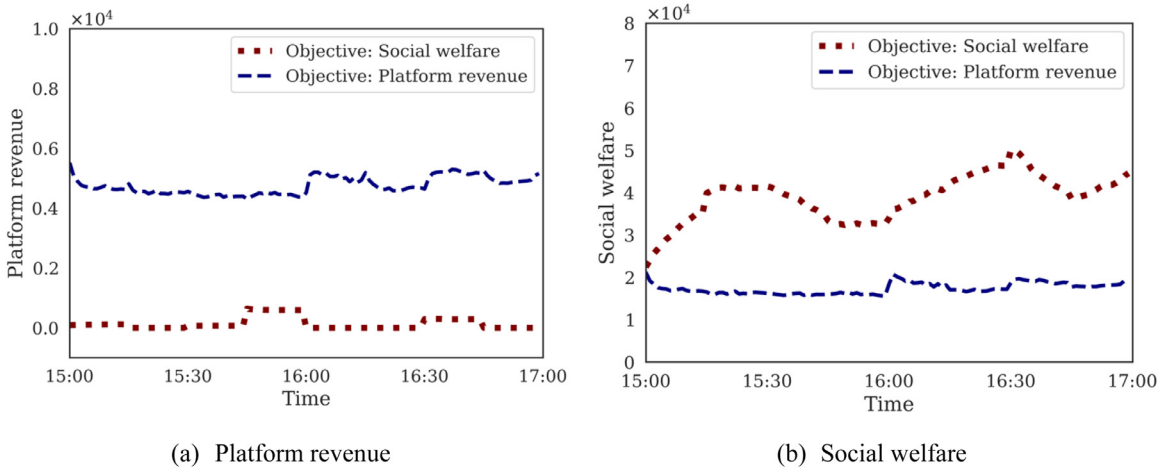

Fig. 10. Objective functions (platform revenue and social welfare) under different dynamic optimization scenarios.

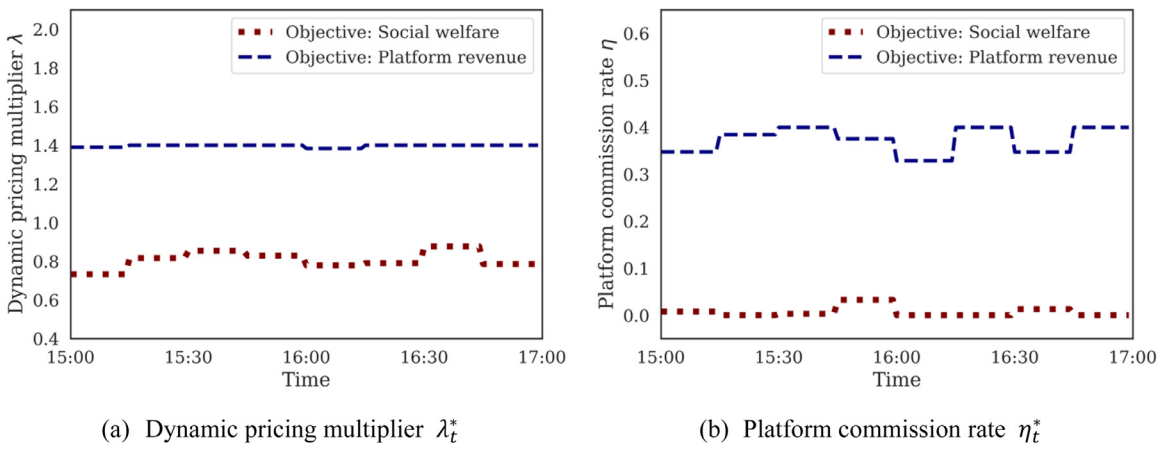

Fig. 11. Decision variables under different dynamic optimization scenarios.

waiting time, there are still a number of drivers entering the market. Therefore, the numbers of waiting vacant cars under the two scenarios in Fig. 12(c) are comparable with each other. The result also shows that passengers are more vulnerable to dynamic optimization strategy's stimulus.

In summary, maximizing one objective function will make various impacts on market performance. For instance, maximizing revenue is beneficial for commercial platforms but may be harmful to the average income of drivers and social welfare. Also, maximizing social welfare is the most balanced strategy for passengers, drivers, and society, while the platform will become a non-profit platform in this circumstance.

6.4. Sensitivity analysis

This section explores the impacts of the optimization constraints and ride-sourcing market parameters. The first part of the optimization constraints includes the decision variable step sizes (constraints 20-21) and lower/upper bounds (constraints 22-23). Among them, $\varepsilon_1, \varepsilon_2, \varepsilon_3, \varepsilon_4$ have specific practical meanings, which represent the maximum acceptance of fluctuations in the trip price and platform commission rate for passengers and drivers, respectively. Therefore, these two constraints are usually decided by the platform. Under the dynamic pricing scenarios, on the one hand, the larger the values of $\varepsilon_1, \varepsilon_2, \varepsilon_3, \varepsilon_4$, the larger the decision space for each optimization process, which may lead to a better result and also make the optimization program not being able to find the optimal solution due to the larger space. On the other hand, lower/upper bounds (i.e., $\lambda^L, \lambda^U, \eta^L, \eta^U$), which are usually controlled by both the platform and government, directly determine the optimization results.

The three dynamic pricing experiments with different step sizes of the decision variables are shown in Fig. 13, more specifically, decision variables in Fig. 13(a) and (b), and objective function in Fig. 13(c). In these three experiments, the objective function is set as the cumulative social welfare. As shown in Fig. 13(c), when the step sizes of the decision variables

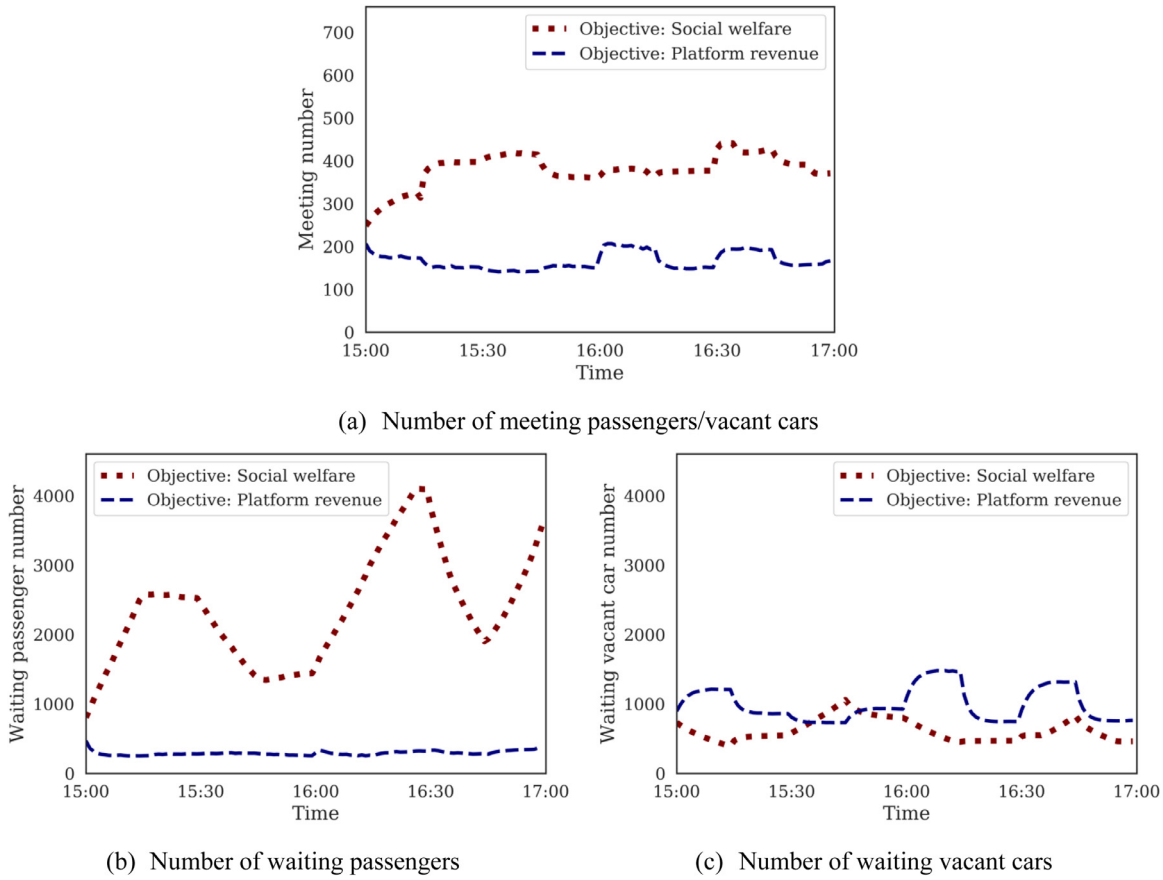

(a) Number of meeting passengers/vacant cars

(b) Number of waiting passengers

(c) Number of waiting vacant cars

Fig. 12. State variables under different dynamic optimization scenarios.

are set the largest, i.e., $\varepsilon_1, \varepsilon_2 = 0.5$, $\varepsilon_3, \varepsilon_4 = 0.2$, the optimization result is not so good as the other two experiments, both of which almost generate the same result. This phenomenon can be explained that the sequential decision problem still cannot be perfectly solved, even when ADP is adopted. However, the power of ADP can be observed when the decision variables show the same trend, as well as the same optimization result in the other two different scenarios.

Fig. 13(d) demonstrates the objective function obtained by the myopic algorithm. Compared with the results of the ADP algorithm in Fig. 13(c), all the three objective functions (myopic) are smaller than the corresponding objective functions (ADP), which once again demonstrates that ADP can significantly increase the objective function compared with the myopic algorithm. Meanwhile, among the three curves in Fig. 13(d), the curve with the smallest values of $\varepsilon_1, \varepsilon_2, \varepsilon_3, \varepsilon_4$ has the highest objective function, then followed by the curves with moderate values and the largest values of $\varepsilon_1, \varepsilon_2, \varepsilon_3, \varepsilon_4$. In the myopic optimization algorithm, the larger decision space means the broader fluctuation range of the decision variables, which may make negative effects on the global optimization result due to the myopic characteristics. In summary, when $\varepsilon_1, \varepsilon_2, \varepsilon_3, \varepsilon_4$ are relatively small, the result of ADP is not sensitive to them, but when they are relatively large, the optimal solution of ADP will decrease slightly (still far superior to the solution of the myopic algorithm).

Next, we test the dynamic pricing scenarios with different lower/upper bounds of the decision variables. Each subfigure in Fig. 14 consists of three pairs of η^L, η^U (x-axis), two pairs of λ^L, λ^U (y-axis), and the objective function (z-axis), which is set as the platform revenue in Fig. 14(a) and social welfare in Fig. 14(b). The sensitivity of different objective functions varies with different lower/upper bounds of the decision variables. Platform revenue, as the objective function, is more sensitive to λ^L, λ^U. As a result, when the feasible range of surge pricing becomes larger or the passenger's incentives are involved, the platform will be more profitable when the optimization goal is platform revenue maximization. It's true that η^L, η^U do influence the optimization performance, however, the influence keeps relatively small (within 4%) if η^L, η^U fluctuate in a reasonable interval based on our numerical results.

Meanwhile, when it comes to social welfare, the objective function's sensitivity to the lower/upper bounds get reversed. Optimized social welfare is more sensitive to η^L, η^U, while only small fluctuations (within 1%) occur as λ^L, λ^U change. That is to say, the enlargement of the commission rate and the introduction of driver incentives can increase social welfare when it is set as the objective function. In summary, the relationship between the optimal objective function and lower/upper

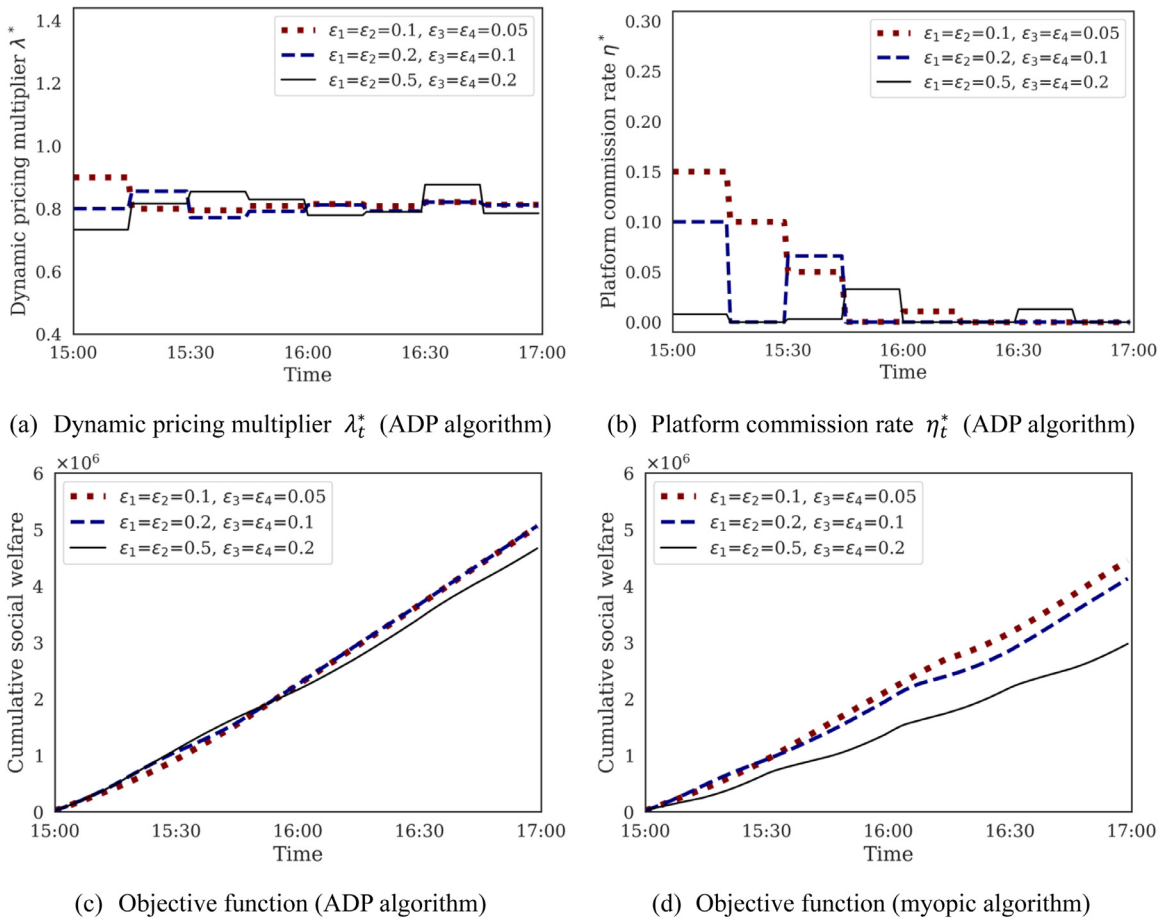

(a) Dynamic pricing multiplier λ_t^* (ADP algorithm)

(b) Platform commission rate η_t^* (ADP algorithm)

(c) Objective function (ADP algorithm)

(d) Objective function (myopic algorithm)

Fig. 13. Dynamic optimization strategies with different step sizes of decision variables (Objective: Social welfare).

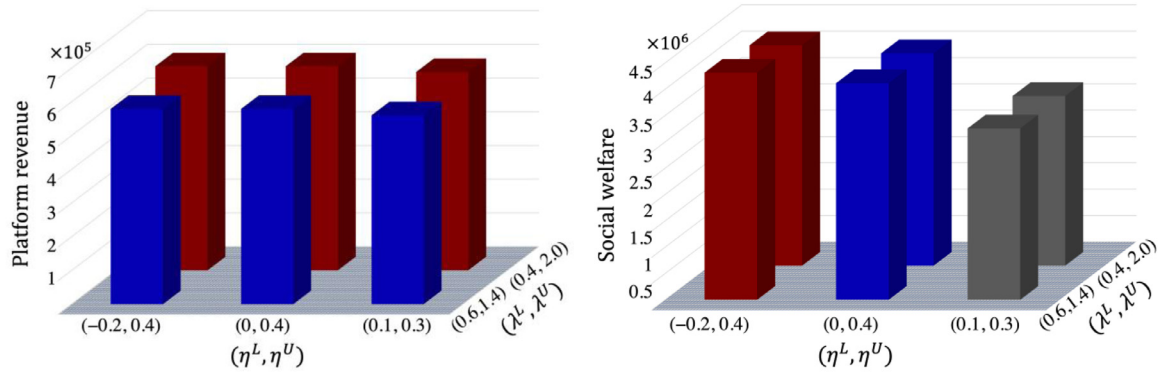

(a) Objective: Platform revenue

(b) Objective: Social welfare

Fig. 14. Dynamic optimization strategies with different decision variables' lower/upper limits.

bounds of the decision variables varies among different types of objective functions, and generally, the broader range of surge pricing and commission rate and the introduction of incentives are helpful to achieve better optimization results.

The second part of the sensitivity analysis is on the ride-sourcing market parameters. Among all parameters of the ride-sourcing market, α_1 and α_2 in the meeting function are the key ones, because they characterize the vacant car-passenger meeting efficiency in the ride-sourcing market. Therefore, we consider four pairs of (α_1, α_2), i.e., (0.45, 0.45), (0.5, 0.5), (0.55, 0.55), and (1, 1), corresponding to decreasing, constant, slight increasing, and largely increasing returns to scale, respectively. To keep the matching function reasonable in the ride-sourcing market with different (α_1, α_2), that is, to maintain the sim-

Table 2
Improved percentage of the objective function by dynamic optimization strategies in different markets

Ride-sourcing markets	(0.45, 0.45)	(0.5, 0.5)	(0.55, 0.55)	(1, 1)
Objective: Platform revenue	78.6%	73.5%	68.9%	47.7%
Objective: Social welfare	57.3%	59.1%	57.2%	62.2%

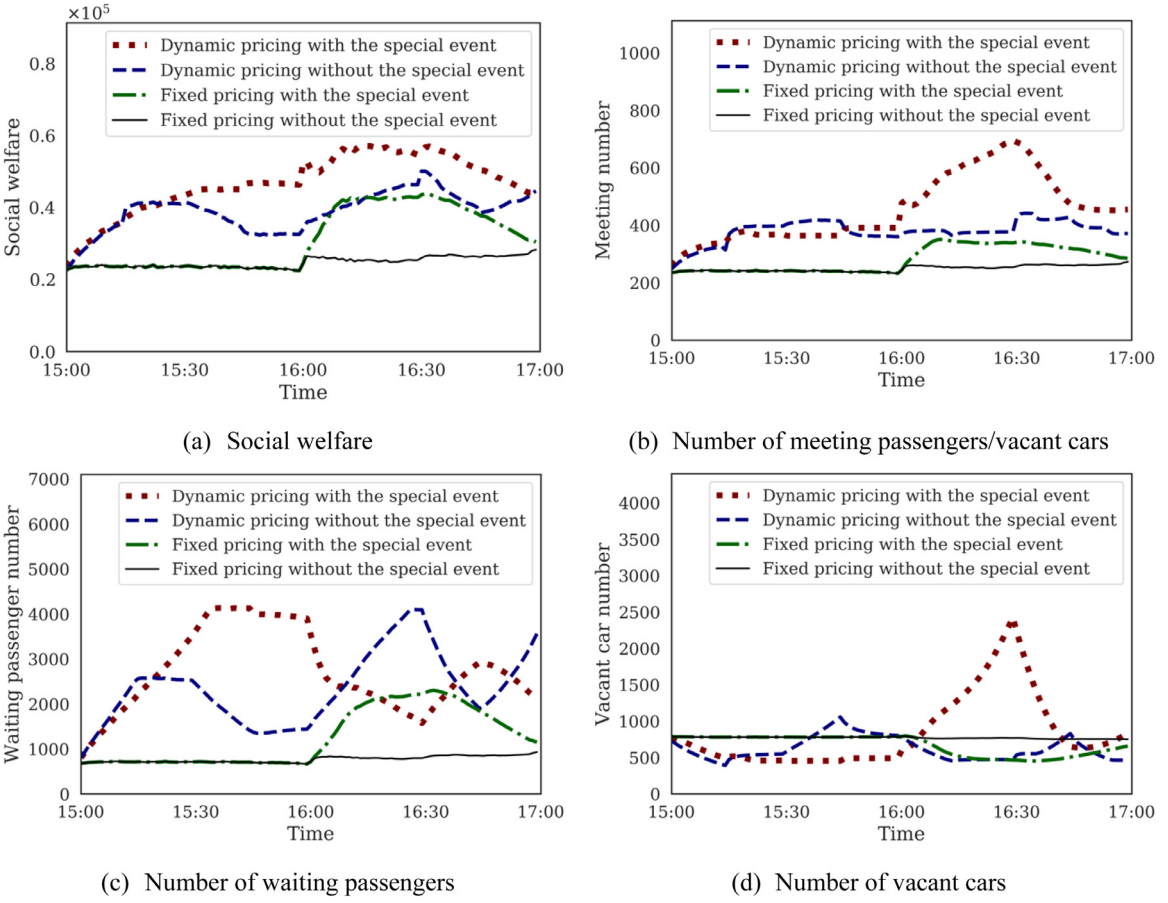

Fig. 15. Social welfare and state variables in a special event under dynamic optimization strategies (Objective: Social welfare).

ulated matching number close to the real matching number, we adjusted some other market parameters accordingly. As a result, we focus on how much dynamic optimization strategies based on ADP can improve the objective function compared with the fixed price in ride-sourcing markets with different matching efficiencies. Table 2 shows the improved percentage of the objective function by dynamic optimization strategies than the fixed-price strategy in markets with different α_1 and α_2. Obviously, dynamic optimization strategies based on ADP can significantly improve the objective function in different market scenarios. When the platform aims to maximize revenue, its performance is the best in the market with decreasing returns to scale and becomes worse in the market with increasing returns to scale. As for the other objective (i.e., social welfare maximization), ADP's performance slightly fluctuates when the ride-sourcing market parameters change.

6.5. Special event experiment

It should be mentioned that the supply and demand data used in this paper are averaged from two-week real-world datasets, which thoroughly describe daily morning/evening peaks and off-peak time periods. However, there will be no visible demand or supply (e.g., a special event) according to the aggregate data. To evaluate the dynamic pricing strategy's effectiveness under a tremendous arrival rate of passengers, we double the potential passenger demand from 16:10 to 16:40, then simulate the two-hour market, in which the special event is included. There are four scenarios in this experiment, namely, fixed price without/with the special event, and dynamic pricing aiming to maximize social welfare without/with the special event. The results are shown in Fig. 15.

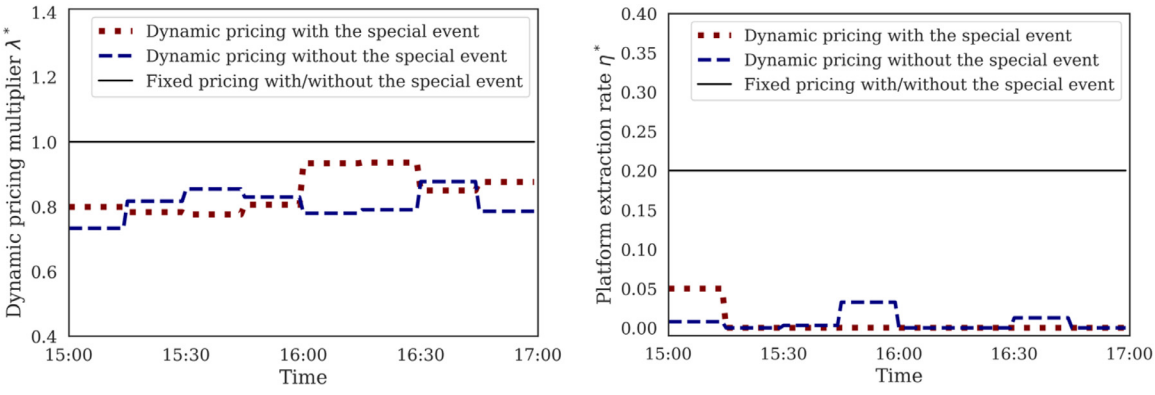

(a) λ_t^* under dynamic optimization strategies (b) η_t^* under dynamic optimization strategies

Fig. 16. Decision variables in a special event under dynamic optimization strategies (Objective: Social welfare).

Observing fixed-price lines without/with the special event (solid black line and dashed dot green line) in Fig. 15(c), we find the impact of current demand on waiting passengers. Under fixed-price scenarios, it should be noted that the number of waiting passengers in the special event is not obtained from the one without the special event according to the aforementioned increased proportion, i.e., doubled potential passenger demand from 16:10 to 16:40. The number is also influenced by two aspects, positively and negatively. On the one hand, more waiting passengers mean the increase of the driver utility, and as more vacant cars enter the market, there will be more passengers attracted. On the other hand, more waiting passengers will also lead to more vacant cars being matched. As a result, there will be fewer vacant cars in the market, i.e., larger passenger's disutility and further fewer passengers in the market. Finally, under the influence of these two effects, the number of waiting passengers in the special event will increase based on the market status. This phenomenon is also reflected in Fig. 15(c), and the solid black line (fixed-price scenario with the special event) is not twice the black dashed line (fixed-price scenario without the special event) from 16:10 to 16:40.

As for the dynamic pricing strategy, we compare it with the fixed-price strategy when the special event occurs. From the results illustrated in Fig. 15(a) and (b), social welfare and the meeting number under the dynamic pricing strategy are always better than those under the fixed-price strategy during regular time periods. Due to the existence of the special event, dynamic pricing even adopts its strategy before the special event to gain more social welfare. During the special event, both social welfare and the meeting number under the dynamic pricing strategy are much better than those during the regular time periods. The number of waiting passengers and vacant cars under the dynamic pricing strategy is influenced more significantly by the dynamic pricing strategy compared to the fixed-price scenario, achieving higher social welfare, which indicates the dynamic pricing strategy outperforms the fixed-price strategy.

In addition, the decision variables λ_t^* and η_t^* of the optimal result are demonstrated in Fig. 16(a) and (b), respectively. The red dotted line and blue dashed line correspond to dynamic pricing scenarios with/without the special event, respectively, while the solid black line is the fixed-price scenario without/with the special event. We can observe that dynamic pricing multiplier λ_t^* is smaller than the fixed-price scenario ($\lambda = 1$), and platform commission rate η_t^* remains zero during the most time, denoted by the blue dashed line in Fig. 16(b). This is because the platform deliberately attracts more passengers and drivers according to the supply and demand situation, to achieve its goal, i.e., social welfare maximization. When the special event occurs, dynamic pricing multiplier λ_t^* increases from 16:00 to 16:30, and platform commission rate η_t^* remains zero.

7. Conclusions

This paper studies several dynamic optimization strategies for the on-demand ride services platform to achieve different targets, in which surge pricing, commission rate, and incentives for passengers and drivers are simultaneously considered. To test the strategies' instant impact on the ride-sourcing market, we propose a dynamic vacant car-passenger meeting model to characterize the influence of optimization strategies on the arrival rate of passengers/vacant cars, the influence of arrival rate of passengers/vacant cars on the waiting numbers of passengers/vacant cars, and the influence of waiting numbers of passengers/vacant cars on the meeting number of passengers/vacant cars. Based on the proposed meeting model, we formulate different optimization problems, i.e., platform revenue maximization and social welfare maximization, from the perspectives of platform and government respectively. A non-myopic ADP algorithm is developed to solve the above sequential decision problems, and a numerical study based on real-world data from an on-demand ride services platform in Hangzhou, China, is conducted to test the optimization strategies and the algorithm. The results show that the ADP-based strategy can achieve better-optimized performance over the myopic strategy, and the platform's oper-

ation target has a significant influence on the structure of the ride-sourcing market. Platform revenue maximization will attract more drivers to provide services, while social welfare maximization will stimulate more passengers to use the platform, in which circumstance the platform almost becomes a non-profit platform. Further, we find that the broader range of surge pricing and commission rate and the introduction of incentives are beneficial to achieve better optimization results.

It should be mentioned that there are still some further research issues on the dynamic optimization strategies for on-demand ride services. For instance, all optimization strategies are determined by the origins of the passengers. However, their destinations are also an essential consideration because the cars need to run empty until meeting the next passengers after serving them. If their destinations' supply is far out of demand, this factor will become even more critical. All these research topics are worthy of investigation in future research.

CRediT authorship contribution statement

Xiqun (Michael) Chen: Conceptualization, Methodology, Supervision, Funding acquisition, Writing - review & editing. **Hongyu Zheng:** Methodology, Data curation, Formal analysis, Validation, Writing - original draft. **Jintao Ke:** Writing - review & editing, Investigation. **Hai Yang:** Methodology, Funding acquisition, Supervision.

Acknowledgments

The first and second authors are supported by the National Key Research and Development Program of China (2018YFB1600900), Zhejiang Provincial Natural Science Foundation of China (LR17E080002), National Natural Science Foundation of China (71771198, 71922019), joint project of National Natural Science Foundation of China and Joint Programming Initiative Urban Europe (NSFC – JPI UE) ('U-PASS', 71961137005), and Young Elite Scientists Sponsorship Program by CAST (2018QNRC001). The third and fourth authors are supported by a grant from the Hong Kong Research Grants Councilunder project HKUST16208619, an NSFC/RGC Joint Researchgrant N_HKUST627/18 (NSFC-RGC 71861167001).

Supplementary materials

Supplementary material associated with this article can be found, in the online version, at doi:10.1016/j.trb.2020.05.005.

Appendix A. Notations

For the convenience of readers, Table A1 lists notations frequently used in the paper.

Table A1
Mathematical notations

Notation	Definition
A	Meeting parameter
c	Minimum wage rate for drivers
C_t	One-stage objective function at time interval t
CM_t	Cumulative meeting number of passengers/vacant cars by time interval t
CQ_t	Cumulative arrival number of passengers by time interval t
CS_t	Consumer surplus at time interval t
CT_t^{vc}	Cumulative arrival number of vacant cars by time interval t
E_d	Price elasticity of demand
E_s	Price elasticity of supply
f	Demand function
F_o	Flag-drop fee
F_t	Travel time-based charge at time interval t
$\overline{F_t}$	Average trip fare at time interval t
g	Supply function
K	Total number of time intervals
l_t	Average passenger's trip time at time interval t
m_t	Meeting rate or departure rate at time interval t
M	Meeting function
n	Time interval length that decision variables change
N_t^{vc}	Waiting number of vacant cars at time interval t
N_t^{p}	Waiting number of passengers at time interval t
PS_t	Producer surplus at time interval t
Q_t	Arrival rate of passengers at time interval t

(*continued on next page*)

Table A1 (*continued*)

Notation	Definition
$\overline{Q_t}$	Potential passenger demand rate at time interval t
R_t	Platform revenue at time interval t
SW	Social welfare
Δt	Time interval length
T_t^{vc}	Arrival rate of vacant cars at time interval t
$\overline{T_t^{vc}}$	Potential vacant car supply rate at time interval t
V_t	Value function at time interval t
$\bar{V}_t$	Value function approximation at time interval t
$\bar{V}_t^n$	Value function approximation of iteration n at time interval t
$\bar{V}_{t,\ N_t^p}$	Value function approximation in terms of N_t^p at time interval t
$\bar{V}_{t,\ N_t^{vc}}$	Value function approximation in terms of N_t^{vc} at time interval t
w_t^p	Passenger's waiting time at time interval t
w_t^{vc}	Vacant car's waiting time at time interval t
α_1, α_2	Elasticities of meeting rate at time interval t
α^n	Learning parameter of VFA in iteration n
β	Monetary value of waiting time
β_0	Monetary value of in-vehicle travel time
δ	Supply scaling parameter
ε_0	Driver's opportunity cost
$\varepsilon_1, \varepsilon_2$	Fluctuation bounds of λ_t
$\varepsilon_3, \varepsilon_4$	Fluctuation bounds of η_t
η_t	Dynamic commission rate at time interval t
η_t^*	Optimal dynamic commission rate at time interval t
η^L, η^U	Lower and upper limits of η_t
θ	Demand scaling parameter
λ_t	Dynamic pricing multiplier at time interval t
λ_t^*	Optimal dynamic pricing multiplier at time interval t
λ^L, λ^U	Lower and upper limits of λ_t
μ_t	Passenger's disutility at time interval t
ν_t	Driver's expected utility at time interval t
φ	Value of operating expense for one car
ω	Unit price of average service time

References

Bai, J., So, K.C., Tang, C.S., Chen, X., Wang, H., 2019. Coordinating supply and demand on an on-demand service platform with impatient customers. Manuf. Serv. Oper. Manage. 21 (3), 556–570.

Banerjee, S., Johari, R., Riquelme, C., 2015. Pricing in ride-sharing platforms: a queueing-theoretic approach. In: Proceedings of the Sixteenth ACM Conference on Economics and Computation, Portland, Oregon, USA, p. 639 -639.

Beesley, M.E., 1973. Regulation of taxis. Econ. J. 83 (329), 150–172.

Beesley, M.E., Glaister, S., 1983. Information for regulating: the case of taxis. Econ. J. 93 (371), 594–615.

Bertsekas, D.P., Tsitsiklis, J.N., 1995. Neuro-dynamic programming: an overview. In: Proceedings of the 34th IEEE Conference on Decision and Control, 1, pp. 560–564.

Cachon, G.P., Daniels, K.M., Lobel, R., 2017. The role of surge pricing on a service platform with self-scheduling capacity. Manuf. Serv. Oper. Manage. 19 (3), 368–384.

Cairns, R.D., Liston-Heyes, C., 1996. Competition and regulation in the taxi industry. J. Public Econ. 59 (1), 1–15.

Chen, H., Zhang, K., Nie, Y.M., Liu, X. (2019). A physical model of street ride-hail. Available at SSRN: https://ssrn.com/abstract=3318557.

Chen, X., Zahiri, M., Zhang, S., 2017. Understanding ridesplitting behavior of on-demand ride services: an ensemble learning approach. Transp. Res. Part C 76, 51–70.

De Vany, A.S., 1975. Capacity utilization under alternative regulatory constraints: an analysis of taxi markets. J. Polit. Economy 83 (1), 83–94.

Douglas, G.W., 1972. Price regulation and optimal service standards: the taxicab industry. J. Transp. Econ. Policy 6 (2), 116–127.

Guda, H., Subramanian, U., 2019. Your Uber is arriving: managing on-demand workers through surge pricing, forecast communication, and worker incentives. Manage. Sci. 65 (5), 1995–2014.

He, F., Shen, Z.M., 2015. Modeling taxi services with smartphone-based e-hailing applications. Transp. Res. Part C 58, 93–106.

Ke, J., Cen, X., Yang, H., Chen, X., Ye, J., 2019. Modelling drivers' working and recharging schedules in a ride-sourcing market with electric vehicles and gasoline vehicles. Transp. Res. Part E 125, 160–180.

Lei, C., Ouyang, Y., 2017. Dynamic pricing and reservation for intelligent urban parking management. Transp. Res. Part C 77, 226–244.

Lei, C., Jiang, Z., Ouyang, Y., 2020. Path-based dynamic pricing for vehicle allocation in ridesharing systems with fully compliant drivers. Transp. Res. Part B 132, 60–75.

Powell, W.B., 2014. Clearing the jungle of stochastic optimization. INFORMS Tutor. Oper. Res. 109–137.

Powell, W.B., Shapiro, J.A., Simao, H.P., 2001. A representational paradigm for dynamic resource transformation problems. Ann. Oper. Res. 104 (1–4), 231–279.

Qian, X., Ukkusuri, S.V., 2017. Time-of-day pricing in taxi markets. IEEE Trans. Intell. Transp. Syst. 18 (6), 1610–1622.

Qian, X., Zhang, W., Ukkusuri, S.V., Yang, C., 2017. Optimal assignment and incentive design in the taxi group ride problem. Transp. Res. Part B 103, 208–226.

Shao, C., Yang, H., Zhang, Y., Ke, J., 2016. A simple reservation and allocation model of shared parking slots. Transp. Res. Part C 71, 303–312.

Varian, H.R., 2004. Microeconomic Analysis, third ed. WW Norton & Company, New York, London.

Wang, X., He, F., Yang, H., Gao, H.O., 2016. Pricing strategies for a taxi-hailing platform. Transp. Res. Part E 93, 212–231.

Wong, K.I., Wong, S.C., Yang, H., 2001. Modeling urban taxi services in congested road networks with elastic demand. Transp. Res. Part B 35 (9), 819–842.

Wong, S.C., Yang, H., 1998. Network model of urban taxi services: Improved algorithm. Transp. Res. Rec. 1623, 27–30.

Yan, C., Zhu, H., Korolko, N., Woodard, D., 2019. Dynamic pricing and matching in ride-hailing platforms. Nav. Res. Logist. doi:10.1002/nav.21872.

Yang, H., Fung, C.S., Wong, K.I., Wong, S.C., 2010a. Nonlinear pricing of taxi services. Transp. Res. Part A 44 (5), 337–348.

Yang, H., Leung, C.W., Wong, S.C., Bell, M.G., 2010b. Equilibria of bilateral taxi-customer searching and meeting on networks. Transp. Res. Part B 44 (8–9), 1067–1083.
Yang, H., Qin, X., Ke, J., Ye, J., 2020a. Optimizing matching time interval and matching radius in on-demand ride-sourcing markets. Transp. Res. Part B 131, 84–105.
Yang, H., Shao, C., Wang, H., Ye, J., 2020b. Integrated reward scheme and surge pricing in a ridesourcing market. Transp. Res. Part B 134, 126–142.
Yang, H., Wong, S.C., 1998. A network model of urban taxi services. Transp. Res. Part B 32 (4), 235–246.
Yang, H., Wong, K.I., Wong, S.C., 2001. Modeling urban taxi services in road networks: Progress, problem and prospect. J. Adv. Transp. 35 (3), 237–258.
Yang, H., Yang, T., 2011. Equilibrium properties of taxi markets with search frictions. Transp. Res. Part B 45, 696–713.
Yang, T., Yang, H., Wong, S.C., 2012. Taxi services with search frictions and congestion externalities. J. Adv. Transp. 48 (6), 575–587.
Yang, T., Yang, H., Wong, S.C., Sze, N.N., 2014. Returns to scale in the production of taxi services: an empirical analysis. Transportmetrica A 10 (9), 775–790.
Yang, H., Ye, M., Tang, W.H.C., Wong, S.C., 2005. A multi-period dynamic model of taxi services with endogenous service intensity. Oper. Res. 53 (3), 501–515.
Zhang, K., Chen, H., Yao, S., Xu, L., Ge, Ji., Liu, X., Nie, Y.M. (2019). An efficiency paradox of uberization. Available at SSRN: https://ssrn.com/abstract=3462912.
Zha, L., Yin, Y., Yang, H., 2016. Economic analysis of ride-sourcing markets. Transp. Res. Part C 71, 249–266.
Zha, L., Yin, Y., Du, Y., 2017. Surge pricing and labor supply in the ride-sourcing market. Transp. Res. Part B 117, 708–722.